Technical University of Liberec
Faculty of Textile Engineering

Fabrication and Characterization of Sutures Made from Composite Nanofibrous Yarns

Divyabharathi Madheswaran

SUMMARY OF THE THESIS
2024

Title of the thesis:	Fabrication and Characterization of Sutures Made from Composite Nanofibrous Yarns
Author:	Divyabharathi Madheswaran
Field of study:	Textile Technics and Materials Engineering
Mode of study:	Full time
Department:	Department of the Nonwovens and Nanofibrous Materials
Supervisor:	Prof. RNDr. David Lukáš, CSc.

Committee for defense of the dissertation:

Chairman:	
Prof. RNDr. Oldřich Jirsák, CSc.	FT TUL, Katedra netkaných textilií a nanovlákenných materiálů
Vice-chairman:	
Prof. Ing. Jakub Wiener, Ph.D.	FT TUL, Katedra materiálového nženýrství
Members of the committee:	
Prof. Ing. Daniela Plachá, Ph.D. (oponent)	VŠB – Technická univerzita Ostrava, CEET
Prof. Ing. Josef Šedlbauer, Ph.D.	FP TUL, Katedra chemie
doc. Ing. Martin Bílek, Ph.D.	FS TUL, Katedra textilních a jednoúčelových strojů
doc. RNDr. Jana Horáková, Ph.D.	FT TUL, Katedra netkaných textilií a nanovlákenných materiálů
Prof. Ing. Ivo Kuřitka, Ph.D. (oponent)	Univerzita Tomáše Bati ve Zlíně, Centrum polymerních systémů

The dissertation is available at the Dean's Office FT TUL.
2024

Abstract

Surgical sutures are widely used biomaterials in healthcare for closing wounds and providing necessary support during healing. However, suture implantation can lead to biofilm formation and infections, resulting in surgical site infections (SSIs), which are the second most common infections in healthcare. Additionally, current commercial sutures are microfibrous assemblies over 10 µm in diameter, failing to replicate the nanoscale structure of the extracellular matrix (ECM). This disparity results in poor cell interactions and suboptimal therapeutic outcomes, particularly for tendons and ligaments. Despite being a critical biomaterial, no groundbreaking advancements have been made to enhance suture multi-functionality or provide nanoscale fibrillar support for cellular activities. This dissertation is an attempt to advance this area of science, research, and development by addressing these gaps and proposing innovative solutions through the development of functional braided composite nanofibrous yarns (CNYs).

The fabrication process involves two steps: first, CNYs with a submicron electrospun sheath on a micro-scale core yarn are produced using alternating current (AC) electrospinning, a technique pioneered by Lukas, Pokorny, and Beran's team, enabling efficient CNY production at 30 m/min. Second, these CNYs are braided to enhance their mechanical properties. The core microfilaments provide mechanical support for wound closure, while the fibrous sheath mimics the ECM, facilitating cellular activities and allowing the incorporation of antibacterial agents like chlorhexidine (CHX) or triclosan (TRC) to accelerate healing.

This dissertation demonstrates the continuous fabrication of various antibacterial braided CNYs. Initial experiments utilized pristine and CHX-loaded polyamide6 (PA6) and polyurethane (PU) electrospun fibers for the sheath layer, with PA micro-yarns as the core. The second approach involved blends of polycaprolactone and polylactic acid (PCL-PLA) and PCL-PLA with CHX or TRC for the sheath layer, using PLA micro-yarns as the core. The third approach employed pristine PCL and PCL with CHX or TRC for the sheath layer and PLA micro-yarns for the core. Morphological assessments confirmed the successful fabrication of CNYs and braided CNYs, while infrared spectroscopy verified the incorporation of CHX or TRC in the yarns. The braided CNYs demonstrated robust breaking forces (29 N) and high thermal stability. Tests for cytotoxicity and antibacterial properties indicated that CHX-loaded PA6 CNY, braided PLA/PCL-PLA CNY, and TRC-loaded PLA/PCL CNY could function as biocompatible, antibacterial surgical sutures.

The outcomes of this research aim to advance surgical techniques and patient care by introducing next-generation sutures with enhanced functionality and antimicrobial capabilities. Additionally, this work sets the stage for future applications in tissue engineering, filtration, wearable electronics, and sensors.

Keywords: AC electrospinning; Braiding; Composite nanofibrous yarn; Core-sheath yarn; Surgical suture.

Abstrakt

Chirurgické nitě jsou ve zdravotnictví široce používané biomateriály pro uzavírání ran a poskytování potřebné podpory při hojení. Implantace stehů však může vést k tvorbě biofilmu a infekcím, což má za následek infekce v místě chirurgického zákrotku (SSI), které jsou druhou nejčastější infekcí ve zdravotnictví. Současné komerční chirurgické nitě jsou navíc mikrovláknové struktury o průměru větším než 10 µm, které nedokážou replikovat strukturu extracelulární matrice (ECM). Tato disparita má za následek špatné buněčné interakce a suboptimální terapeutické výsledky, zejména u šlach a vazů. Navzdory tomu, že jde o kriticky důležitý biomateriál, dosud nebyly provedeny žádné převratné pokroky, které by zlepšily multifunkčnost chirurgických nití nebo poskytly fibrilární podporu na buněčné úrovni. Tato disertační práce je pokusem o pokrok v této oblasti, a předkládá možné řešení těchto nedostatků a navrhuje inovativní řešení prostřednictvím vývoje funkčních pletených kompozitních nanovlákenných přízí (CNY).

Výrobní proces zahrnuje dva kroky: za prvé, CNY se submikronovým pláštěm na mikrovlákenné jádrové přízi, jsou vyrobeny pomocí elektrického zvlákňování střídavým proudem (AC), což je nový způsob výroby nanovlákenných materiálů vyvinutý Lukašem, Pokorným a Beranem. Tento způsob výroby umožňuje efektivní produkci CNY při 30 m/min. Za druhé, aby bylo dosaženo lepších mechanické vlastnosti, jsou CNY splétány ve výsledné nitě. Mikrovlákenné jádro CNY poskytuje potřebnou pevnost pro uzavření rány, zatímco vlákenná obálka napodobuje ECM, podporuje buněčné aktivity a umožňuje začlenění antibakteriálních látek, jako je chlorhexidin (CHX) nebo triclosan (TRC), pro urychlení hojení.

Tato disertační práce demonstruje kontinuální výrobu různých antibakteriálních splétaných CNY. V počátečních experimentech byla vlákenná obálka kompozitní příze připravena z polyamidu-6 (PA6), PA6 s chlorhexidinem a polyuretanu (PU), a PA mikrovlákny jako jádrem. Druhý přístup zahrnoval směsi polykaprolaktonu a kyseliny polymléčné (PCL-PLA) a PCL-PLA s CHX nebo TRC pro vlákennou obálku s použitím mikrovlákenných přízí z PLA jako jádra. Třetí přístup využíval PCL a PCL s CHX nebo TRC pro vlákennou obálku a PLA mikrovlákna pro jádro. Morfologická hodnocení potvrdila úspěšnou výrobu CNY a splétaných CNY, zatímco infračervená spektroskopie ověřila začlenění CHX nebo TRC do přízí. Opletené CNY prokázaly dostatečnou pevnost (29 N) a vysokou tepelnou stabilitu. Testy cytotoxicity a antibakteriální aktivity ukázaly, že chlorhexidinem funkcionalizované PA6 CNY, splétané PLA/PCL-PLA CNY a triclosanem funkcionalizované PLA/PCL CNY by mohly fungovat jako biokompatibilní antibakteriální chirurgické šicí materiály.

Výsledky tohoto výzkumu představují pokrok v péči o pacienty zavedením chirurgických nití nové generace se zvýšenou funkčností a antimikrobiálními vlastnostmi. Tato práce navíc připravuje „půdu“ pro budoucí aplikace v tkáňovém inženýrství, filtraci, nositelné elektronice a senzorech.

Klíčová slova: AC electrospinning; Splétání; Kompozitní nanovlákenná příze; Příze jádro-plášť; Chirurgická nit'.

Contents

List of Figures

List of Tables

List of Abbreviations

1D ..... One dimensional

2D ..... Two dimensional

AC ..... Alternating current

BSA ..... Bovine serum albumin

CHX ..... Chlorhexidine

CNY ..... Composite nanofibrous yarn

DC ..... Direct current

DCM ..... Dichloromethane

DMEM ..... Dulbecco's modified Eagle medium

DMF ..... Dimethylformamide

DTG ..... Differential thermogravimetric analysis

ECM ..... Extracellular matrix

EDS ..... Energy dispersive X-ray spectroscopy

E. coli ..... Escherichia coli

EU ..... European Union

F ..... Formic acid

FA ..... Formic acid/acetic acid

FAA ..... Formic acid/acetic acid/acetone

FTIR ..... Fourier-transform infrared spectroscopy

HPLC ..... High-performance liquid chromatography

MTT ..... 3-(4,5-Dimethylthiazol-2-yl)-2,5-Diphenyltetrazolium Bromide

PA6 ..... Polyamide 6

PCL ..... Polycaprolactone

PLA ..... Polylactic acid

PU ..... Polyurethane

RPM ..... Revolutions per minute

SEM ..... Scanning electron microscope

SSI ..... Surgical site infections

S. aureus .... Staphylococcus aureus

TGA ..... Thermogravimetric analysis

TRC ..... Triclosan

US ..... United States

XPS ..... X–ray photoelectron spectroscopy

1. Introduction

The origin of yarn is still unknown, but it has a long and fascinating history. According to yarn artifacts excavated worldwide, the earliest evidence of human-made yarn (flax fiber), dating back 27,000 years, has been found in the Czech Republic [1]. This suggests that the region has been engaged in yarn production since ancient times. The history of surgical yarns (or sutures) in medical therapeutics can be traced back thousands of years, during which Egyptians, Indians, and other early pioneers in suture development utilized easily accessible materials like silk, linen, cotton, horsehair, gold thread, and various animal tendons and intestines (catgut) [2]. The natural sutures offer several advantages, including biodegradability and ease of handling. However, they also present certain drawbacks, such as contributing to post-operative infection, which leads to delays in wound healing, as well as limitations in availability and variability [3].

Synthetic sutures emerged as a result of advancements in material science and the desire to overcome certain limitations associated with natural sutures. The introduction of synthetic non-degradable (or non-absorbable) polymeric sutures, such as nylon, polypropylene, polyester, and steel wire, during and after the World War II greatly expanded the use of suture materials [3]. The benefits of non-absorbable sutures include long-term wound support, which reduces the likelihood of suture failure and enhances durability, knot security, and versatility. However, a drawback of non-absorbable sutures is their inability to degrade naturally and necessitate subsequent surgery for removal. To counter these challenges, the development of absorbable (degradable) synthetic sutures began in the later part of the 20^{th} century, such as polyglycolic acid, polylactic acid, and polydioxanone. The benefits of absorbable suture materials are that they degrade within the body through enzymatic processes or hydrolysis, so secondary surgery procedure is avoided. They also provide a predictable absorption rate and versatility. So, synthetic absorbable sutures have received significant attention in the biomedical field compared to non-absorbable suture materials [3, 4].

Statistical data indicates that sutures account for 57% of the global market for surgical devices [5]. The global market value of surgical sutures was estimated to be 4 billion USD in 2023 and it was expected to surpass 5.5 billion USD by 2028 [6]. The clinical data suggested that sutures have been playing a vital role in saving patients' lives and/or improving their quality of life, but some drawbacks of sutures have to be addressed.

1.1 Overview of the current state of the problem

Commercially available sutures comprised of microfibers with a diameter of typically more than 10 μm, which is larger than the extracellular macromolecules (protein fibrils) presented in the extracellular matrix (ECM). The ECM provides structural and biochemical support to the surrounding cells, also it governs the cellular activities (adhesion, proliferation, cell-communication, and differentiation) [7, 8]. Consequently, the disparity in fiber morphology and size between suture materials and ECM constituents inevitably leads to unfavorable cell interactions and therapeutic outcomes [9].

Furthermore, sutures are considered foreign materials to the host body, which can lead to the formation of biofilm and related infections, which later become surgical site infections (SSI). SSI is the second most common infection in the healthcare sector [10, 11]. In the European Union (EU) and the United States (US), approximately 20% of the 4.1 million and approximately 15% of the 2.4 million cases of nosocomial infection are associated with SSIs [12, 13]. Post-surgical infections often result in prolonged hospital stays and may necessitate additional surgery, thereby increasing healthcare costs. Conventional oral antibiotic therapy, typically effective for minor bacterial infections, often proves inadequate for treating SSIs due to the rapid formation of biofilm on wound suture surfaces. In light of these challenges, the prevention of SSIs and improving the wound healing process are imperative, a goal that can be achieved through the development of antibacterial functionalized nanofibrous sutures [14].

The functionalization of suture can be performed by using a post-fabrication coating technology to deposit antimicrobial agents onto the surface of pristine wound sutures. However, the poor control over coating thickness and antibacterial agent release are notable drawbacks of this coating process, despite its simplicity and cost-effectiveness. Ideally, the antibacterial agents should thus be incorporated during the fabrication process, which is more straightforward compared to the post-fabrication treatment of sutures. Unfortunately, melt-spinning technology, which is the most widely applied technique for commercial suture production, utilizes a high temperature to melt the starting polymer. This high temperature strongly impedes the use of thermal-sensitive antibacterial agents in the suture production process [15].

In recent years, many scientists have proposed nanofibrous yarn or 1D electrospun fibrous bundle as a surgical suture, which was directly transferred from the 2D electrospun fibers produced by electrospinning technology into the textile yarn-like linear assembly [8, 16–18]. Electrospinning involves the electrohydrodynamic phenomenon, where an electrified polymeric solution or melt is elongated into a continuous jet and then undergoes diverse electrohydrodynamic instabilities (such as stretching and bending or whipping instabilities) within an electric field. In solution electrospinning, the jet experiences rapid solvent evaporation as it moves toward the counter electrode, forming solidified electrospun fibers. In the case of melt electrospinning, the solidification process occurs as a result of heat transfer between the molten jet and the surrounding ambient air [19, 20].

The inherent properties of electrospun fibers, such as interconnected ultrafine fibrous structure, nanoscal size, high surface-to-volume ratio, porosity, and ECM nanofibril-mimicking characteristics, make electrospun nanofibrous yarn an ideal material for surgical suture applications [8]. In addition, functional components such as antibacterial agents, anti-inflammatory substances, growth factors, and analgesics can be easily loaded into the electrospun yarn through electrospinning technology and/or post-treatment processes. Thus, localized drug delivery is an additional advantage of these materials. These capabilities accelerate the wound-healing process. However, inherently poor mechanical properties of nanofiber yarn strongly restrict their use as wound sutures [21]. Some researchers have attempted to address this issue by improving the mechanical properties of nanofiber-based yarns through techniques such as twisting and hot stretching [22, 23]. Still, these methods often compromise the overall porosity of the material.

Researchers have recently addressed this issue by fabricating composite nanofibrous yarns (CNYs) or core-sheath electrospun nanofibrous yarns [24]. These yarns consist of a core-shell structure; the shell layer comprises nanofiber, while the core layer comprises classic yarn or microfilaments. The core microfilaments provide the necessary mechanical supports to keep the incision closed and hold the wound's surrounding tissues together. As previously mentioned, the fibrous sheath provides the necessary functionality and facilitates cellular activities. Nevertheless, fabricating microfilament coated with electrospun nanofibrous (core-shell) yarn using the existing direct-current-based (DC) electrospinning technologies poses a technological challenge, requiring an electrically active or grounded collector to collect the charged electrospun fibers. Due to the repulsion caused by like charges, the polymer jet spreads out, resulting in fibers being deposited over a larger area. Therefore, depositing the electrospun fibers onto the electrically neutral core yarn to create CNY proves to be challenging. Furthermore, the deposition of electrospun fibers is significantly influenced by the collector's geometry and position [19, 25].

To overcome this particular shortcoming of DC electrospinning technology, Lukas, Beran, Pokorny and their co-workers have developed an alternating current (AC) electrospinning process [26–29]. From a technological point of view, both AC and DC electrospinning are similar. However, AC electrospinning significantly differs from DC in terms of the polarity of applied high-voltage, which is the function of time. Additionally, AC potential builds a virtual collector a few centimeters away from the spinning electrode [30]. Due to the rapid polarity changes, the polymeric liquid and subsequent polymeric jet and electrospun fibrous segments simultaneously experience positive and negative charge polarities. The emerging fibrous segments are neutralized once they reach the virtual collector, and subsequently, fibrous segments are interconnected. These interconnected fibers further grow from the virtual collector with the help of the surrounding electric wind.

Therefore, unlike DC, AC high-voltage creates a mechanically compact interconnected fibrous structure, so-called electrically neutral fibrous plume. Due to the AC electrospun mechanical compactness and charge neutrality, it can be easily manipulated using other technologies. For instance, fibrous plumes can be easily twisted into 1D nanofibrous bundles using a twisting device, it can be easily coated on the classic yarn to make composite nanofibrous yarn, and it can be directly deposited on rotating collector to make 2D electrospun membranes [30–37]. In the case of CNYs, the production rate can be up to 60 m/min, depending upon the polymer, technological, and ambient parameters [34]. While composite nanofibrous yarn exhibits combined functionality and acceptable mechanical properties, their structural integrity and the weak adhesive force between the core and nanofibrous sheath impede their utilization as mechanically robust functional surgical sutures.

To address this issue, for the first time this PhD work propose a method to fabricate functional braided nanofibrous composite yarns as the next generation surgical sutures. It is dual step process, initially composite nanofibrous yarns, featuring a submicron electrospun sheath coated on a micro-scale core yarn was prepared by advanced AC electrospinning. In the second step, as-fabricated CNYs were braided using braiding technology to enhance the overall mechanical properties and functionality of these yarns.

1.2 Purpose and aim of the thesis

To address SSI, improve the wound-healing process, and provide the necessary mechanical support, this study proposes a method for preparing various functional braided CNYs for surgical suture applications. Initially, various pristine and functional CNYs were fabricated using free-surface collectorless AC electrospinning. Subsequently, as-fabricated CNYs were braided using braiding technology to enhance their overall mechanical properties. Therefore, the objectives of this thesis are directed towards the following aspects.

❶ **Fabrication of braided functional composite nanofibrous yarn.**
The primary objective was to develop a novel approach for fabricating functional braided CNYs using AC electrospinning and braiding technology. This involves coating microscale yarns with nanofibers through AC electrospinning and subsequently braiding the CNYs to create braided CNYs structures suitable for surgical sutures (Fig. 1.1).

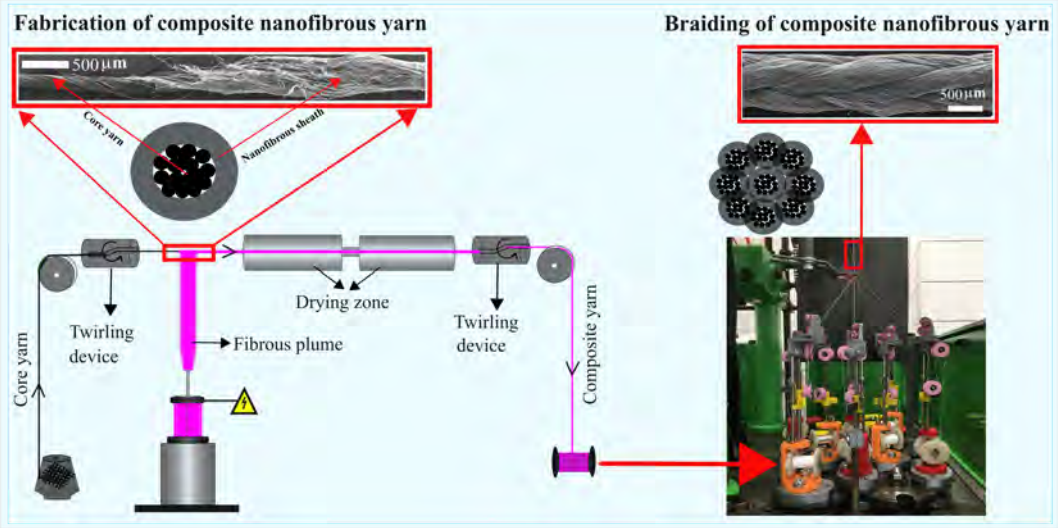

Figure 1.1: *The braided CNY preparation process using AC electrospinning and braiding technology.*

A few specific problems of this objective are,

- ❍ Since large-scale production of CNYs using conventional electrospinning techniques remains technologically challenging, CNYs are produced by AC electrospinning technology. Unlike DC electrospinning, optimized solvents are not available for AC electrospinning. Therefore, this study finds an optimized solvent for various polymers (polycaprolactone (PCL), blends of polycaprolactone-polylactic acid (PCL-PLA), polyurethane (PU), and polyamide6 (PA6)).
- ❍ Since braiding is a mechanical process, maintaining the structural integrity of the electrospun fibrous sheath during the braiding process presents additional challenges.

❷ **Study the morphological, physicochemical, mechanical, and thermal properties of braided yarns.**
This objective aims to comprehensively characterize the as-fabricated yarns to evaluate their morphological, physicochemical, mechanical, and thermal properties. Scanning Electron Microscopy (SEM) was utilized to analyze the surface morphology and structural integrity of the CNYs and braided CNYs. The gravimetric scale was used to determine the linear density, providing insights into the mass per unit length of the yarns. Fourier-Transform Infrared Spectroscopy (FTIR) was employed to assess the chemical composition and identify functional groups, thereby offering a detailed understanding of the physicochemical properties. Thermogravimetric Analysis (TGA) was conducted to evaluate the thermal stability of the as-fabricated yarns, highlighting their degradation behavior under temperature variations. Following TGA, tensile testing was performed to measure the maximum breaking force and extension, offering crucial data on the mechanical robustness and flexibility of both the CNYs and braided CNYs under stress.

❸ **Investigate the antibacterial activity and biocompatibility of braided yarns.**
The third objective is to evaluate the functional properties of the braided yarns, including their antibacterial activity and biocompatibility. The antibacterial activity of the braided yarns was assessed against *Staphylococcus aureus* (*S. aureus*) and *Escherichia coli* (*E. coli*) using the agar diffusion test to measure inhibition zones, indicating the effectiveness of the antibacterial agents incorporated into the yarns. Chlorhexidine (CHX) and triclosan (TRC) served as model antibacterial agents and are known for their efficiency against a wide range of microorganisms and biocompatibility. The biocompatibility of the yarns was investigated using the MTT assay with fibroblast cells to ensure that the yarns are non-cytotoxic and support cellular activities that are critical for tissue healing.

1.3 Significance of the thesis

The significance of this thesis lies in its potential to advance the field of surgical wound closure by introducing a novel approach that harnesses the unique properties of nanofiber coatings. By improving cell interaction, reducing the risk of infection, and enhancing mechanical properties, nanofiber-coated sutures have the potential to revolutionize surgical techniques and improve patient outcomes across a wide range of surgical specialties. This research contributes to our understanding of biomaterial-based approaches to wound healing and lays the foundation for the development of next-generation surgical sutures with enhanced functionality and efficacy. Also, the proposed method offers a versatile approach for producing various functional braided CNYs applicable in tissue engineering scaffolds, filters, wearable electronics, and sensors.

2. Materials and Methods

This chapter intends to give the reader a comprehensive overview of the materials and the strategic methodology employed to accomplish the goals of the Ph.D. dissertation.

2.1 Materials

Polyurethane (PU, Mw = 2000 g/mol, Larithane LS 1086) and Polyamide 6 (PA6, Mw = 66360 g/mol, Ultramid B27 01) were purchased from Novotex BASF. Polycaprolactone (PCL, Mw= 45000 and 80000 g/mol), and antimicrobial agent (chlorhexidine (CHX), triclosan (TRC)) were purchased from Sigma-Aldrich. Polylactic acid (PLA) (Ingeo^{TM} biopolymer 4043D) was purchased from Natureworks. Polycaprolactone (PCL, Mw= 50000 g/mol) purchased from CAPA. Materials for biocompatibility or cytotoxicity, such as 3-(4,5-Dimethylthiazol-2-yl)-2,5-Diphenyltetrazolium Bromide (MTT), bovine serum albumin (BSA), Dulbecco's modified Eagle medium (DMEM), phalloidin-fluorescein isothiocyanate, Triton-X-100, and 4',6 diamidine-2-phenylindole (DAPI) were also purchased from Sigma Aldrich.

Dimethylformamide (DMF) (99.5%), formic acid (F, 98%), acetic acid (A, 99%), acetone (Ac, 99%), dichloromethane (DCM), sulfuric acid (96%), and sodium chloride were obtained from PENTA. PA6 commercial yarn (to act as core yarn) with a linear density of 46 dtex/12 filaments was provided by Odetka s.r.o and PLA commercial yarn (to act as core yarn) with a linear density of 250 dtex was provided by Sintex s.r.o. Silicone mold was provided by Czech Academy of Sciences. All the materials were used as received.

2.2 Spinning solution preparation

This section explains the various polymeric solution preparation used in this study. The polymer concentration and the composition of spinning solutions are listed in Table 2.1.

Preparation of pristine and antibacterial PU and PA6 solution

Pristine solutions of PU (15 wt%) and PA6 (10 wt%) were prepared using DMF and a mixture of formic acid/acetic acid (1:1 v/v) as solvents, respectively. To fabricate antibacterial yarns, the antimicrobial agent CHX (0.75 wt%) was added to the prepared pristine PU and PA6 solutions. Additionally, to improve the electrospinnability of the PA6 solutions, sulfuric acid was added (0.2 mol/L) to both the PA6 and PA6-CHX solutions. All solutions were stirred overnight at room temperature until a homogeneous solution was obtained. The obtained results of these solution were discussed in section 3.1.

Preparation of pristine and antibacterial PCL-PLA solution

To prepare a blend PCL-PLA precursor solution, 5 wt % PCL, 2 wt % PLA, and 0.5 wt % NaCl were dissolved in DCM. To prepare a drug-loaded solution, 1 wt % CHX or TRC, 5 wt % PCL, and 2 wt % PLA were dissolved in DCM, so-called PCL-PLA-CHX or PCL-PLA-TRC. All solutions were stirred overnight at room temperature. The obtained results of these solution were presented in section 3.2.

Table 2.1: *Summary of prepared polymeric solutions with respect to their section number. Abbrivation: PU = Polyurethane, PA6 = Polyamide 6, PCL = Polycaprolactone, PLA = Polylactic acid, CHX = Chlorhexidine, TRC = Triclosan. DMF = Dimethylformamide, F = Formic acid, A = Acetic acid, A_c = Acetone, DCM = Dichloromethane, H_2SO_4 = sulfuric acid, NaCl = sodium chloride.*

Section	**Spinning solution**	**Polymer**	**Drug**	**Solvents/additives**	**polymer concentration [Wt%]**
3.1	PU	PU	-	DMF	15
	PU-CHX	PU	CHX	DMF	15
	PA6	PA6	-	FA/H_2SO_4	10
	PA6-CHX	PA6	CHX	FA/H_2SO_4	10
3.2	PCL-PLA	PCL, PLA	-	DCM/NaCl	7
	PCL-PLA-CHX	PCL, PLA	CHX	DCM	7
	PCL-PLA-TRC	PCL, PLA	TRC	DCM	7
3.3	PCL	PCL	-	FAA_c	11
	PCL-CHX	PCL	CHX	FAA_c	11
	PCL-TRC	PCL	TRC	FAA_c	11

Preparation of pristine and antibacterial PCL solution

Pristine solution of PCL spinning solution (Mw = 45000 and 80000 g/mol at the ratio of 1:3 w/w) was prepared using the combination of formic acid, acetic acid, and acetone 1:1:1 (v/v) to attain 11 wt% (w/v). Meanwhile, to prepare the antibacterial solution, the antibacterial agent of CHX (0.5 wt%) and TRC (0.5 wt%) was added to the pristine PCL solution. All solutions were stirred overnight at room temperature. The obtained results of these solution were presented in section 3.3.

2.3 Experimental methods

This section describes the AC electrospinning setup and braiding machine setup. Using these combinations of setups, first, produce the nanofiber-covered composite yarn by AC electrospinning using various polymeric solutions; then, the obtained composite yarns were braided using the custom built-braiding machine to prevent the abrasion-resistance and improve the mechanical property.

2.3.1 Composite nanofibrous yarns (CNYs) fabrication using AC electrospinning

The fabrication of composite nanofibrous yarn is schematically represented in Fig. 2.1. A rod spinneret (length: 10 cm, diameter of the head: 2 cm) was fused into the solution reservoir with a custom-designed screw pump (Technical University of Liberec, Czech Republic). The prepared polymer solution was fed by the screw pump to the spinneret head through the coaxial channel. The speed of the screw pump (frequency) was maintained at 500 RPM to feed approximately 18 ml/min of the solution to the spinneret to

achieve a stable plume of nanofibers. Once the electric potential was applied to the spinneret, a compact fibrous plume was generated due to the charge polarity. The AC voltage with sinus waveform was generated by a KGUG 36 (Asea Brown Boveri - Switzerland) high-voltage transformer (conversion ratio of 36000 V/230 V). An ESS 104 variable autotransformer (Thalheimer Transformatorenwerke Gmbh - Germany) was used to control the output and input voltage of 0-250 V and 230 V, respectively. The effective voltage for all conducted experiments is given in Table. 2.2.

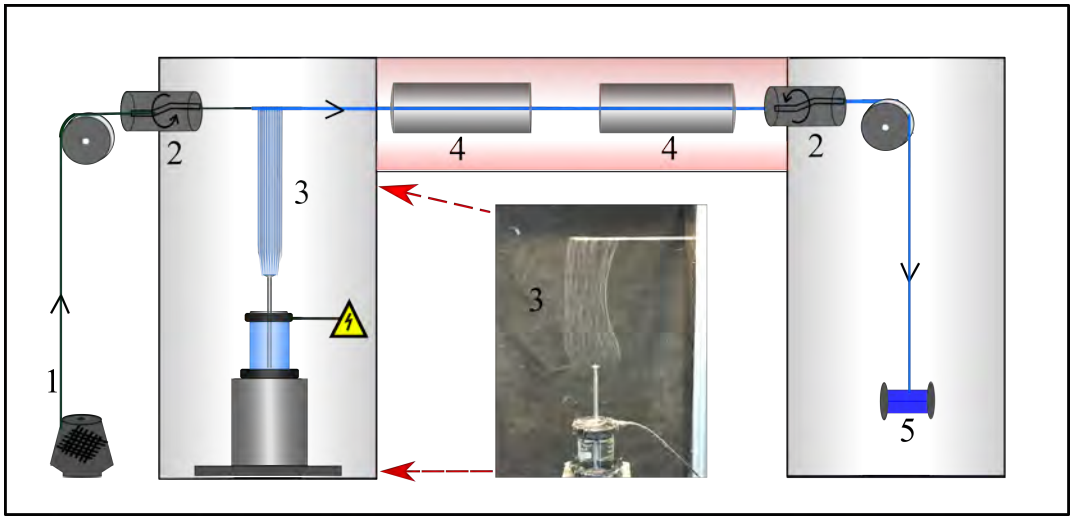

Figure 2.1: *Schematic representation of the AC electrospinning device. 1. core yarn, 2. twirling device, 3. plume of nanofibers being coated around the core yarn, 4. drying zone, 5. composite nanofibrous yarn.*

The aforementioned fibrous plume moved forward in the vertical direction because of the electric wind. The plume of nanofibers was wrapped on the core yarn by axial rotation and ballooning of the yarn by a set of two twirling devices, which are rotating in the same direction (front and rear). The first twirling device was placed before the spinning zone, and the second one was placed after a set of two drying zones (length of 2.2 m) which provided sufficient drying of residual solvents from the nanofibrous sheath. Subsequently, compacted composite yarns were collected on the output bobbin. The inner and outer diameters of both drying zones (a hot air blower Mistral 6 - Leister Technologies AG - Switzerland) were 3 cm and 5.5 cm, respectively. The spinning conditions for all the samples are listed in Table 2.2.

Table 2.2: *Summary of spinning condition.*

Section	**Core yarn**	**Nanofibrous envelope**	**Applied voltage** [kV]	**Frequency** [Hz]	**Winding speed** [m/min]	**1^{st} Twirling device** [RPM]	**2^{nd} Twirling device** [RPM]	**Drying zone** [°C]	**Humidity** [%]
3.1	PA6	PU	32	50	20	3000	3000	95	36
	PA6	PU-CHX	32	50	20	3000	3000	95	36
	PA6	PA6	32	50	10	3000	3000	95	36
	PA6	PA6-CHX	32	50	10	3000	3000	95	36
3.2	PLA	PCL-PLA	38	50	30	10000	10000	50	50
	PLA	PCL-PLA-CHX	38	50	30	10000	10000	50	50
	PLA	PCL-PLA-TRC	38	50	30	10000	10000	50	50
3.3	PLA	PCL	35	50	12	6000	5000	40	60
	PLA	PCL-CHX	35	50	12	6000	5000	40	60
	PLA	PCL-TRC	35	50	12	6000	5000	40	60

2.3.2 Fabrication of braided composite nanofibrous yarns

Braided yarns were produced using an HC Taiwan braiding machine [Model EY-RA-8-4(110 II)] with an 8-carrier arrangement Fig. 2.2a and b. The commercial yarn carrier was modified by installing a series of ceramic pulleys and ceramic eyelets on the channel to produce the braided CNY without harming the fibrous coating (Fig. 2.2c). Half of the carriers move in a clockwise direction, while the other half move in an anticlockwise direction (Fig. 2.2e). This motion creates the characteristic interlacement pattern of the braid, which is continuously formed during the braiding process to produce a continuous length of braided material. To achieve this interlacement pattern, the braiding machine employs a series of horn gears arranged on a track. Each bobbin is mounted on a carrier that engages with the slots of the horn gears and is transferred from one horn gear to the next (Fig. 2.2d and e). This transfer is facilitated by a mechanism that acts like a railroad switch and includes cam surfaces that hold the carriers against the horn gears. Consequently, each bobbin follows a serpentine path, with half traveling clockwise and the other half counterclockwise. The braided yarns interlace when the bobbin carriers cross over each other.

Figure 2.2: *Images of the braiding machine and its components. (a) The braiding machine, (b) a close-up view of the yarn braiding process, (c) commercial yarn carriers (left) and custom-built yarn carriers (right, green circle highlights the modifications), (d) horn dog with a carrier, (e) arrangement of horn gears (black and blue lines indicate the path of the horn dog with the carrier), and (f) pawl (circle) and ratchet (rectangle).*

The bobbin carrier mechanism is crucial for maintaining constant yarn tension and allowing the yarns to feed or retract as needed. During braiding, carriers adjust their distance to the convergence point in the braiding plane. As they approach the convergence point, the carriers retract the previously fed yarn to prevent slackness. The yarns pass

from the bobbins over a set of spring-loaded pulleys, forming a reservoir length, and then through an exit guide. A pawl and ratchet system prevents the bobbins from rotating. Yarn is either fed from the reservoir or retracted into it by deflecting a spring-loaded pulley. When the reservoir length is exhausted, the yarn tension increases momentarily, triggering the pawl to release the ratchet, which feeds new yarn into the reservoir, repeating the process (Fig. 2.2f). The required retraction length ranges from 3 to 12 cm.

The CNYs were mounted on each custom-build carrier of the braiding machine (8 carriers plus 1 central carrier) to create braided CNY. The production rate for braided CNYs was 0.25 m/min. Each composite yarn was maintained under a tension of 30–32 cN during the braiding process to ensure a compact braided structure. The production rate for braided yarns was 15 m/h at a frequency of 22 Hz for all samples.

2.4 Characterizations

This section outlines the various characterization techniques employed in this study, including SEM, FTIR,XPS, HPLC, linear density measurement, tensile strength testing, TGA, abrasion testing, antibacterial testing, and cytotoxicity assessment.

2.4.1 Scanning electron microscopy analysis

The surface morphology of composite and braided yarns were determined using a Tescan (VEGA3 Czech Republic) SEM at an accelerating voltage of 20 kV. Prior to the analysis, all samples were sputter-coated with a 7 nm thin layer of gold by using a Quorum (Q150R ES) sputter coater. The average diameter of the braided yarns (n=20 measurements) and electrospun fibers (100 measurements) was measured by ImageJ software. In addition, elemental mapping and elemental composition percentage of the braided yarns were also investigated with energy-dispersive X-ray spectroscopy (EDS) (S3700N) present on the Zeiss Ultra Plus-FE-SEM (Germany). The SEM images of as-fabricated yarns are shown in Fig. 3.1 on page 15, Fig. 3.7 on page 24, and Fig. 3.13 on page 30. The obtained from EDS are shown in Fig. 3.15 on page 32.

2.4.2 Linear density

The linear density of composite and braided yarns in dtex was analyzed by using a gravimetric method. For this analysis, 1 meter of the sample was weighed with an analytical balance. Subsequently, dtex was calculated by using the following formula:

$$\text{Linear density (dtex)} = \frac{\text{mass of the 1 m yarn (g)}}{\text{length of the 1 m yarn (m)}} \times 10000 \tag{2.1}$$

The linear density of various fabricated CNYs and braided CNYs are shown in Fig. 3.3 on page 19, Fig. 3.8 on page 25, and Fig. 3.14 on page 31.

2.4.3 Fourier-transform infrared spectroscopy analysis

The functional group of composite and braided yarns was analyzed by FTIR (Nico-let iZ10, Thermo Fisher Scientific, USA) spectrometer equipped with a single reflection attenuated

total reflection (ATR) accessory using a diamond crystal as the internal reflection element. The FT-IR spectra were recorded in the range of 4000 - 700 cm^{-1}, at a resolution of 4 cm^{-1}. The FTIR spectrs are presented in Fig. 3.2 on page 17, Fig. 3.9 on page 26, and Fig. 3.16 on page 33.

2.4.4 High-performance liquid chromatography analysis

The amount of CHX in the PU and PA6-CHX Composite yarns was quantified by HPLC. First, PU-CHX (length: 2 m and weight: 133 mg) or PA6-CHX (length: 2 m and weight: 110 mg) CNYs were dissolved in 200 µL of DMF or formic acid, respectively. Subsequently, the CNY-containing liquids were vortexed for 2 min, after which 800 µL of water was added to precipitate the polymer. The resulting CHX-containing solutions were analyzed by using a Dionex Ultimate 3000 HPLC system. The separation was performed on a Phenomenex Kinetex EVO C18 column with a length of 150 mm, an inner diameter of 4.6 mm, and a particle size of 2.6 µm. The measurements were performed under an isocratic regime using 70% aqueous mobile phase and 30% organic components. The aqueous component of the mobile phase consisted of 50 mM H_3PO_4. in 5% acetonitrile, and the organic component was pure acetonitrile. The flow rate of each sample was maintained at 1.5 mL/min, and the column oven temperature was set to 40 °C. The volume of injected samples was set at 20 µL followed by the filtration process using nylon syringe filters with 13 mm diameter and 0.22 µm pore size. The chromatograms were recorded at a wavelength of 258 nm for 3 min. The resulting amount of CHX is presented as the average over 2 measurements from the obtained CNY-derived solution. The HPLC chromatograms are shown in Fig. 3.2 on page 17.

2.4.5 X-ray photoelectron spectroscopy analysis

XPS surface analysis was performed using a PHI 5000 Versaprobe II spectrometer equipped with a monochromatic Al K_α X-ray source (h = 1486.6 eV) operating at 25 W. During the XPS spectral acquisition, the pressure in the chamber was maintained below 10^{-6} Pa for pristine and drug-loaded PU and PA6 composite nanofibrous yarn samples. Survey scans were recorded with a pass energy of 187.85 eV (step size = 0.8 eV) at an angle of 45° with respect to the normal of the sample. The XPS results are shown in Fig. 3.2 on page 17.

2.4.6 Mechanical properties

The tensile strength of the CNYs was evaluated by a tensile machine (LaborTech 2.050, Czech Republic) with a gauge length of 10 cm and a displacement rate of 10 cm/min. The CNY was vertically mounted into the clamps of the dynamometer. LabTest v.3 software was used to construct the force vs. deformation curves of the samples during the measurements. From these curves, the tensile strength was determined. A minimum of ten measurements was performed for each condition. (This method was used only for PU- and PA6- based composite nanofibrous yarn; Fig. 3.3 on page 19).

The tensile strength of the braided CNYs was evaluated by a tensile machine (Testometric, UK) with a gauge length of 10 cm and a displacement rate of 3 cm/min. The braided yarns were vertically mounted into the clamps of the dynamometer. A minimum

of five measurements was performed per sample. This method was used only for PCL and PCL-PLA braided CNYs. The mechanical properties, including the maximum breaking force and extension, of the braided CNYs are illustrated in Fig. 3.11 on page 28 and Fig. 3.18 on page 35.

2.4.7 Thermogravimetric analysis

To analyze the thermal stability of the different CNYs and braided CNYs, TGA experiments were performed by using a thermogravimeter TGA 2 (Mettler Toledo, Switzerland). The samples were heated from 50-600 °C at a heating rate of 10 °C/min under a nitrogen atmosphere at a nitrogen flow rate of 50 mL/min. The decomposition temperature at maximal weight loss rate (Tmax), which corresponds to the inflection point of the TGA curve, was determined from the derivative thermogravimetric (DTG) curve. TGA results are shown in Fig. 3.4 on page 21, Fig.3.10 on page 27 and Fig. 3.17 on page 34.

2.4.8 Abrasion test

The adhesion of the nanofibrous envelope to the core yarn was evaluated by using a custom-assembled device that is shown in Fig. 2.3. The device consisted of the following four components: (1) spring, (2) winding shaft device, (3) knitting needle eyelet, and (4) calibrated tension sensor with a measuring range of 0-1000 cN (VUTS a.s, Czechia).

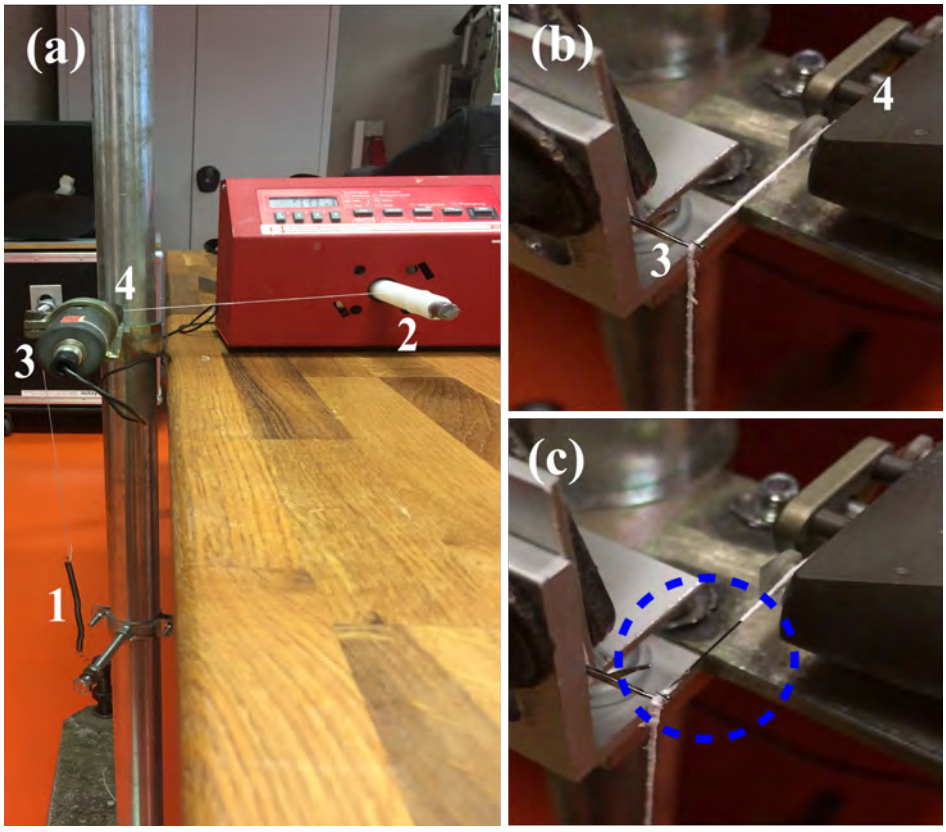

Figure 2.3: *(a) Front view of the core-envelope adhesion measuring device setup: 1. Spring, 2. winding shaft, 3. knitting needle eyelet, 4. tension sensor; (b) detailed top view of a CNY passing through the knitting needle and tension sensor, and (c) the fibers envelope (white) detachment from the core yarn (black yarn), shown in the blue circle.*

For each measurement, a yarn was cut into a piece with a length of approximately 1 m. Subsequently, one end of the yarn was connected to the spring eyelet, while the other end was fastened to the winding shaft. In between the spring and the winding shaft, the yarn passes through a knitting needle eyelet, after which the angular displacement of the yarn changes to 90°. The calibrated yarn tension sensor was placed close to the needle eyelet in the direction of the winding device. During the measurement, the yarn was wound around the winding shaft at a constant velocity (10 m/min). At the same time, the tensile force of the yarn increased due to the elongation of the spring until the nanofiber envelope is broken. At the moment of the initial damage of the nanofiber envelope, the tensile force value was determined with the tension sensor by using MGCplus AB22A software. For each CNY, four measurements were carried out. The results obtained from this experiment is presented in Fig. 3.3 on page 19. This method was used only for PU- and PA6- based CNYs. In the case of braided CNY, it was not possible to measure it due to the low sensitivity of the tension sensor.

To assess the wear resistance of the nanofibrous envelope during sewing, an abrasion test was conducted on the resultant braided yarns, including PLA/PCL, and CHX or TRC loaded PLA/PCL. The following methods were employed: 1) sewing the yarns onto a silicone mold, 2) sewing the yarns onto a silicone mold with a drop of phosphate-buffered saline (PBS), and 3) sewing the yarns onto a chicken thigh. These methods were specifically designed by the author due to the lack of standardized testing protocols for such studies.

Figure 2.4: *(a) Setup of the abrasion experiment using silicone mold with PBS, (b) incision of chicken thigh, and (c) stitched incision using various resultant braided yarns.*

Fig. 2.4a illustrates the experimental setup for the abrasion test using the silicone mold, which had a width of 0.6 mm. The abrasion experiments with the silicone mold were performed in two different ways: i) the braided CNY were gently penetrated through the dry silicone mold, and ii) the braided CNY were penetrated through the silicone mold, on which a drop of PBS was placed. For the third method, a chicken thigh was selected as the test medium, purchased from a supermarket, and used for the experiments within 2 hours of purchase. A 5.5 cm incision was made on the chicken thigh, as shown in Figure 2.4b. The incision was then stitched using the PLA/PCL, PLA/PCL-CHX, and PLA/PCL-TRC braided yarns, with their respective images presented in Figure 2.4c.

2.4.9 Antibacterial test

In order to evaluate the antibacterial properties of the composite and braided yarns, agar diffusion tests with *S. aureus* and *E. coli* (CCM 3954, Masaryk University, Czech Republic) were performed. Bacterial suspensions were grown overnight on nutrient broth at 37 °C. Prior to the experiments, the turbidity of the overnight cultured sample was adjusted to a standardized optical density value of 0.1 at 600 nm. Subsequently, for composite yarns, four vertical lines of freshly prepared bacterial culture were smeared on agar plates. To determine the inhibition zone, pristine and antibacterial-loaded PU and PA6 composite yarns with a length and width of ≈7 cm and 3 mm, respectively, were placed in the horizontal direction. After 24 hours of incubation at 37 °C, the zone of inhibition was measured for at least 3 samples per condition. For braided yarns, the culture was spread evenly over the surface of trypticase soy broth agar (Himedia, India) plates using a sterile paper cotton swab. The pristine and antibacterial-loaded PCL braided yarns (length: 5 cm) were placed at the centre of the agar plates. After that, all agar plates were incubated at 37 °C for 24 hours. The zone of inhibition was measured for each sample at least 10 times. The obtained results from this analysis is depicted in Fig. 3.5 on page 22, Fig. 3.12 on page 29, and Fig. 3.20 on page 37.

2.4.10 Cytotoxicity test

The cytocompatibility of various composite and braided yarns was analyzed by using a standard MTT assay with 3T3-SA mouse fibroblasts cells. In short, all the samples were sterilized by ethylene oxide using an Anprolene AN-74i sterilizer prior to the MTT tests. Subsequently, the culture medium was exposed to the resultant braided yarns for 24 hours at 37 °C, after which the obtained liquid was brought in contact with the fibroblasts for 24 hours at 37 °C. Then, the cell viability was assessed by a MTT assay and compared to the cell viability of fibroblasts exposed to a normal culture medium (control).

On the first day, fibroblasts cells (passage 23) were seeded in 96 well microtiter plates at a density of 10000 cells/100 μL per well and cultured for 24 hours. The cells were cultured in Dulbecco's modified eagle medium-high glucose (DMEM, Sigma) supplemented with 10% of fetal bovine serum (FBS, Biosera) and 1% antibiotic-penicillin & streptomycin amphotericin B (Lonza Biotec) in a humidified atmosphere incubator under 5% CO_2 at a temperature of 37 °C. The same day, braided yarns were placed in 24 well plates, followed by the addition of 1 mL of complete culture medium. Subsequently, the samples were incubated for 24 hours at 37 °C. During the second day, the culture medium was removed from the cell-seeded 96 well plates. Immediately thereafter, 100 μL of the culture medium from the braided yarns containing 24 well plates were extracted and added to the fibroblast-containing wells. After incubation at 37 °C for 24 hours, the cytotoxicity of the braided yarns derived culture medium was examined by a colorimetric MTT assay. Therefore, the culture medium was first removed, after which 200 μL of the MTT solution was added to each well and incubated for 3 hours. Then, 200 μL of isopropyl alcohol was added to each well, and the UV absorbance was measured at 570 nm by using a Spark multi-mode micro-plate reader. The complete culture medium is considered as control, and all measurements are normalized to the cell metabolic activity of the control. The results are presented as an average over 7 measurements. The obtained results are depicted in Fig. 3.6 on page 23, Fig. 3.12 on page 29, and Fig. 3.20 on page 37.

3. Obtained results

3.1 Fabrication of chlorhexidine-loaded PU and PA6 CNYs

This sub-chapter 3.1 investigates the production of pristine and antibacterial CNYs using a PA6 core yarn with a PU or PA6 electrospun sheath produced by the advanced collectorless AC electrospinning. The morphological and physicochemical properties of these yarns are analyzed using various characterization techniques, including SEM, XPS, FTIR Spectroscopy, and HPLC. The mechanical properties are assessed through tensile testing, and the adhesion force of the electrospun sheath to the core yarn is measured. Additionally, the thermal stability of the yarns is evaluated using TGA. Finally, the antibacterial properties and biocompatibility were examined through the MTT assay and the agar diffusion method, respectively.

3.1.1 Spinnability and surface morphology of CNYs

The surface topography of the different CNYs as evaluated by SEM was depicted in Fig. 3.1. Fig. 3.1a clearly shows that the PU nanofibers are completely wound around the PA6 core yarn. This is caused by the ability of the pristine PU solution to form a continuous thick fibrous plume that can be wrapped onto the running core yarn, resulting in the formation of the desired core-envelope yarn or CNYs. Fig 3.1e clearly shows that PU nanofibers can be formed by AC electrospinning with the employed DMF-based solution, which further expands the polymer range for this method [30, 34, 35, 38, 39].

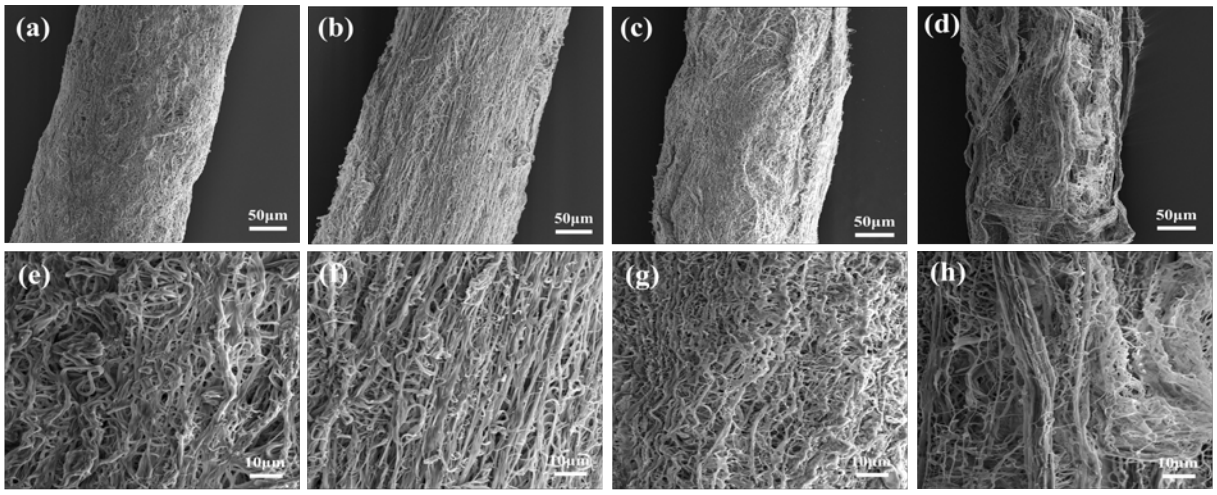

Figure 3.1: *SEM images of the different CNYs at different magnifications: a) and e) PU, b) and f) PU-CHX, c) and g) PA6, and d) and h) PA6-CHX.*

The addition of CHX into the PU solution did not impair the electrospinning process, and PU-CHX composite yarns could be prepared under the same spinning condition. The resulting PU-CHX CNY also has an envelope that is completely wound around the PA6 core yarn and that is uniformly oriented along the core yarn axis. Valtera et al. demonstrated that the rotational speed of the second twirling device is essential to obtain the desired fiber orientation [34]. As such, it can be concluded that an angular speed of

3000 RPM results in the formation of nice core-sheath yarns. By comparing the high-resolution SEM images (Fig. 3.1e-f), it could be observed that the nanofibers in the envelope were more straightened for the PU-CHX CNY than for the pristine PU CNY. Similar behavior was observed before by Rysanek et al., who observed that the addition of CHX to a PA6 electrospinning solution resulted in straighter fibers [40]. By combining experimental data and modeling, they indicated that the molecular interactions of the CHX with the polymer chains were responsible for the altered nanofiber morphology [41, 42].

In contrast to the PU solution, the PA6 solution required the addition of sulfuric acid to form stable fibrous plumes under AC conditions. This is in line with previous observations from Kalous et al., who reported that the addition of an acid to the PA6 polymeric solution increases its conductivity, which is necessary to allow the formation of a stable fibrous plume during the AC electrospinning process [35]. The addition of 0.2 mol/L of sulphuric acid facilitated the formation of a nanofibrous envelope structure that is shown in Fig. 3.1c and g. It is clear that the nanofibers are completely wound around and uniformly oriented along the core yarn axis, similar to what was observed for the PU and PU-CHX CNYs. The addition of CHX into the PA6 solution did not impair the electrospinning process, but a more randomly deposited bunch of similar and thicker fiber segments is observed in comparison to the PA CNYs. This is most likely related to the increase in conductivity of the electrospinning solution due to the addition of CHX. This results in an increased charge density on the polymer jets, which can result in a stronger combination of repulsion and attraction in between the jet segments due to the AC voltage [43]. This could in turn lead to the formation of a bunch of thicker fibrous strands in the fibrous plume. Similar to the PU-CHX CNY, also the PA6-CHX CNYs are straighter than the PA6 CNY. This can be again attributed to the interaction between the CHX molecules and the polymer chains.

As such, for both the PU and PA6 solutions, it can be concluded that the addition of CHX resulted in the formation of CNYs with a clear fibrous envelope. The differences in nanofiber alignment and morphology in between the pristine and CHX-based CNYs reveal that the addition of CHX has an effect on the electrospinning process, which already suggests that some CHX molecules are introduced in the CNYs.

3.1.2 Chemical analysis of the CNYs and quantification of incorporated CHX in the CNYs

The chemistry of the resultant CNYs was examined by ATR-FTIR (Fig. 3.2a). The FTIR spectrum of PU shows contributions that can be expected based on its chemical structure. Among the most prominent contributions, a first peak can be observed at 3336 cm^{-1}, which can be attributed to the N-H stretching vibration originating from the carbamate group in the polymer. Two other peaks at 2939 cm^{-1} and 2857 cm^{-1} can be related to the C-H asymmetric and symmetric stretching, respectively, originating from the -CH_2- groups in the polymer backbone. Other significant contributions from the carbamate group can be observed at 1741 cm^{-1} (C=O stretching), 1558 cm^{-1} (N-H bending & C-N stretching), and 1244 cm^{-1} (C-N stretching). Additionally, a contribution at 1066 cm^{-1} can be associated with asymmetric C-O-C stretching [44–46]. The addition

of CHX to the spinning solution did not result in the addition of new peaks in the FTIR spectra of the resulting CNYs, as the spectrum of PU-CHX was similar to the spectrum of pristine PU.

However, the spectrum of the PU-CHX CNYs shows some small differences as compared to the spectrum of the PU CNYs, as the N-H and C=O stretching peaks are shifted to 1552 and 1640 cm^{-1}, respectively. This indicates that the amount of incorporated CHX is low, as CHX addition to other materials usually resulted in more significant changes [47, 48]. However, a similar behavior was observed for dental cement, as the addition of the antibacterial agent benzalkonium chloride did not result in changes in the FTIR spectrum, although it made the material antibacterial [49]. The small shifts could probably be attributed to the interaction of the CHX molecules and the PU.

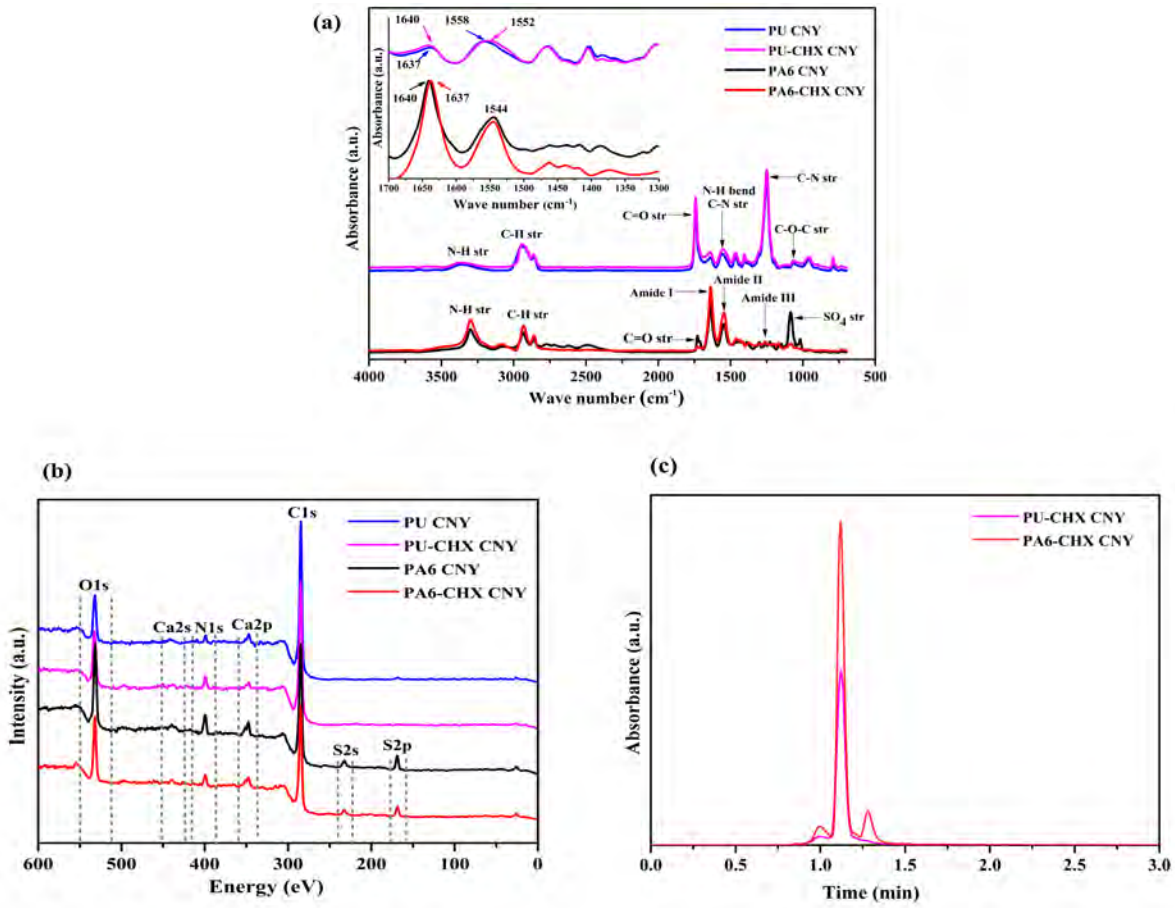

Figure 3.2: *ATR-FTIR (a) and XPS survey (b) spectra of the different CNYs, and chromatograms (c) of the solution of the PU-CHX and PA6-CHX CNYs.*

The FTIR spectrum of the PA6 CNY also shows contributions that can be expected based on its chemical structure (Fig. 3.2a). The most prominent contributions of the secondary amide can be observed at 3298 cm^{-1} (N-H stretching), 1640 cm^{-1} (C=O stretching, amide I band) and 1544 cm^{-1} (N-H bending and C-N stretching, amide II band), 1261cm^{-1} (C-N stretching, amide III bands) [46]. The aliphatic chain results in the main contribution at 2931 and 2859 cm^{-1} (asymmetric and symmetric C-H stretching, respectively) and smaller peaks at 1462 and 1416 cm^{-1} (C-H bending vibrations). The additional peak that appeared at 1728 cm^{-1} could be attributed to the absorption of C=O from the by-products

of the acid-catalyzed amide hydrolytic degradation which was initiated by formic, acetic, and sulfuric acid [50, 51]. During the degradation process of PA6, oligomers in different lengths and monomers in the form of ions can be formed [52, 53]. Hence, the C=O band at 1728 cm^{-1} could be originated from ketone, ester, carboxylic acid, or imide groups, which can be formed after the scission of the amide group [50, 54]. As expected, SO_4 stretching present in sulfate ions can also be observed at 1084 cm^{-1} due to the addition of sulfuric acid in the PA6 based spinning solutions [55].

It can also be observed that the FTIR spectra of the PU and PA6 CNYs are completely different, which can be expected because the nanofibrous sheath is thicker than the FTIR analysis depth, which is in the order of 700 nm [56]. Therefore, no contribution of the PA6 core yarn is observed. The PA6-CHX CNY shows mainly a difference for the hydrolysis and sulfuric acid-related peaks, as the contributions at 1728 and 1084 cm^{-1} are significantly decreased. This suggests that the addition of CHX may lead to occurring interactions between CHX on the one hand and hydrolysis products and sulfuric acid on the other hand resulting into a decreased contribution of the stretching vibrations of the latter molecules. Additionally, the PA6-CHX CNY also shows a slight shift of the amide I peak to 1637 cm^{-1} and a small alteration in the amide II peak at 1544 cm^{-1}, similar to what was observed for the PU-CHX sample. This suggests that the amount of incorporated CHX is also low for the PA6 CNYs.

This hypothesis is additionally supported by XPS measurements, which were used to study the surface elemental composition of the materials. Fig. 3.2b compares an XPS survey scan of the PU and PA6 CNYs and their CHX-based counterparts. No peak corresponding to chlorine can be observed for both materials, which shows that the amount of CHX on the surface of the materials is below the XPS detection limit. This is similar to observations of Rysanek et al., who observed no chlorine for CHX-containing PA6 nanofibers [41]. Besides the absence of a contribution of chlorine, carbon, oxygen, nitrogen, and calcium atoms can be observed for the PU and PU-CHX CNYs. The first three atoms can be expected based on the chemical structure of the polymer, while the calcium atoms are the result of contamination due to sample handling. For the PA6 and PA6-CHX CNYs, the same atoms can be observed, but also a contribution of sulfur can be observed. This is in line with the observations in ATR-FTIR, which suggested that sulfate ions were introduced in the CNYs. As such, it can be concluded that the amount of CHX in the CNYs is low, as only minor differences can be observed in the FTIR spectra.

To gather more information on the amount of incorporated CHX in the CNYs, HPLC was performed on solutions obtained after dissolving the CNYs. The chromatograms (Fig. 3.2c) of the dissolved PU-CHX and PA6-CHX CNYs both show a clear peak around 1.1 min retention time, which clearly corresponded to the CHX in the solution, as confirmed by the calibration curve that was made for different CHX concentrations (see supporting information). For the PU-CHX CNYs, a CHX concentration of 22.0 ± 1.1 mg/L was obtained, which corresponds to 11.0 ± 0.6 µg of CHX per meter of yarn. The concentration for the PA6-CHX CNYs was 48.0 ± 2.2 mg/L, which corresponds to 23.8 ± 1.1 µg/m. Apparently, the amount of incorporated CHX is higher for the PA6-based CNYs, although the same amount of CHX (0.75 wt%) was added to the polymeric solutions. This could be related to the difference in wt% in the electrospinning solutions (PU: 15 wt% and

PA6: 10 wt%), making the relative amount of CHX compared to the polymer mass in the solution higher for PA6, which could be transferred to the resulting CNYs. However, also other properties of the spinning solution, such as the solvent, the conductivity can have an influence. It should be noted that increasing the CHX concentration in the electrospinning solution to increase the resulting amount of CHX in CNYs is not possible because it impairs the AC electrospinning process.

3.1.3 Linear density and mechanical properties

The linear density of the different CNYs was calculated by using a gravimetric method, as explained in section 2.4.2, and the results are shown in Fig. 3.3a. The linear density of the composite PU yarn is 88 dtex in which 42 dtex (48%) is occupied by the nanofibrous envelope, and the remaining 46 dtex (52%) is occupied by the core yarn, while the PU-CHX CNY has a nanofibrous envelope of 21 dtex (31%) and a core yarn of 46 dtex (69%). For the PA6 CNY, the linear density is 69 dtex in which 23 dtex (34%) is occupied by the nanofibrous envelope, while the PA6-CHX CNY consists of 11 dtex (19%) of nanofibers that are coated on the core yarn of 46 dtex (81%). It is known that the linear density of envelope nanofibers is inversely proportional to the velocity of the core yarn [57, 58]. If the velocity of the core yarn is reduced, the available time for nanofiber deposition will be increased, and consequently, a larger amount of nanofibers will be wounded around the core yarn. However, as a constant velocity is used during the electrospinning process, the linear density analysis clearly shows that the PU electrospinning results in a higher nanofiber throughput than the PA6 electrospinning.

For both polymers, the addition of CHX results in a significantly reduced productivity of electrospun fiber fabrication (50%). This could be attributed to the increased conductivity of the polymeric solution upon the addition of CHX. However, due to the limited knowledge on the fundamental concepts of the AC electrospinning process, it is difficult to get a deeper insight in this result.

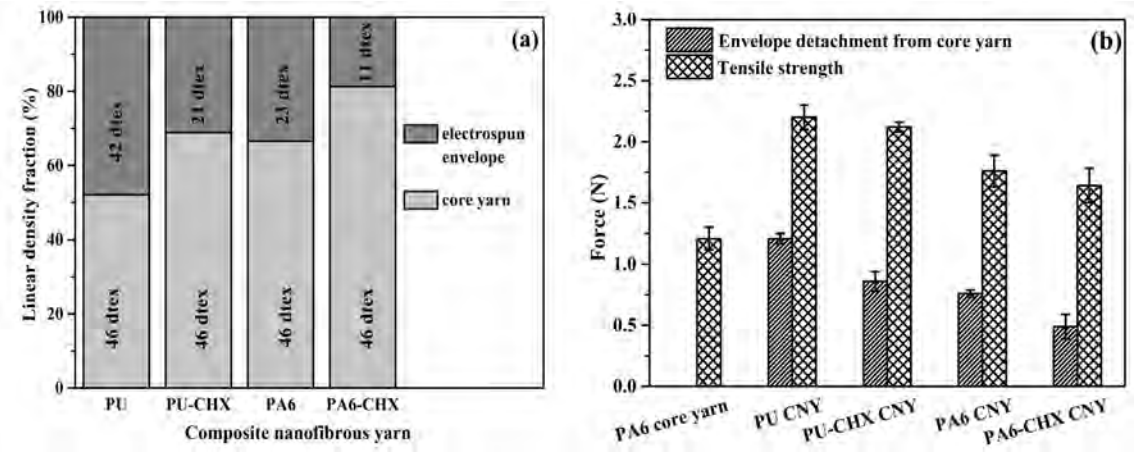

Figure 3.3: *(a) Linear density of CNYs, and (b) the force values at which the electrospun envelope was detached from the core yarn and the tensile strength of the yarns.*

The adhesion of the electrospun envelope to the core yarn was tested as described in section 2.4.8. The corresponding force values are presented in Fig. 3.3b. The envelope adhesion to the core yarn was higher for the PU CNY than for PU-CHX CNY, suggesting

that the CHX addition influences the attachment between core and envelope. Generally, the adhesion between these two polymers can result from a variety of different interaction forces, such as Van Der Waals and/or electrostatic forces [34, 59]. Exactly estimating the influence of these forces is, however, outside of the scope of this article. The PA6 CNY shows a very similar adhesion as the PU-CHX CNY, as a non-significant difference in the detachment force is observed. The addition of the CHX in the PA6 solution results in CNYs with lower detachment force as compared to the PA6 CNYs. This seems to indicate that the linear density of the envelope has an influence on its detachment, as the PU CNY performs better than the PU-CHX and PA6 CNYs, which have a similar envelope linear density and detachment force, while the PA6-CHX CNYs have the lowest envelope linear density and detachment force. This indicates that a higher amount of envelope material results in a higher force that is needed to remove this nanofibrous envelope. Additionally, the high-resolution SEM images indicated that the PU and PA6 envelope nanofibers were twisted to a greater extent than their CHX-containing counterpart, which could also increase the adhesion to the core.

The tensile strength of the core and composite yarns, which was measured as described in section 2.4.6, is also shown in Fig. 3.3b. These results clearly show that the tensile strength of the composite yarns was significantly higher than the tensile strength of the core yarn. The cohesive force between the nanofibers in the envelope provides additional strength to the CNYs, which results in their improved mechanical properties. Overall, the PU-based CNYs perform better than the PA6-based CNYs, which can be related to the better mechanical properties of the former polymer in comparison to the latter [60]. The addition of the CHX in the polymer envelope does not result in a significant change in the tensile strength. This suggests that the overall material properties are more important for the resulting mechanical property of the CNY than the linear density and envelope adhesion force, as the CHX addition resulted in a decrease of the latter CNY properties. Moreover, the PU- and PA6-CHX CNYs still have a higher tensile strength than the PA6 core yarn, indicating that these CHX-containing core-sheath-based materials have superior mechanical properties.

3.1.4 Thermal properties of the CNYs

The thermal degradation process of the PA6 core yarn and the fabricated CNYs were evaluated by TGA. The TGA thermograms, the corresponding DTG curves and the Tmax values are shown in Fig. 3.4. Fig. 3.4 shows that the core yarn loses weight below 100 °C, which is most likely related to the hygroscopic nature of PA6, as previous studies have highlighted the sensitivity of this material to moisture [61, 62]. After this initial weight loss, the polymer remains stable until ± 350 °C, and the decomposition has a Tmax of 438 °C. For the PU-based CNYs, a completely different behavior is observed. No weight loss is observed until ± 300 °C, indicating that the nanofibrous shell around the core yarn prevents a significant amount of moisture adsorption by the PA6 core yarn. The PU CNY shows a significant weight loss starting from 300 °C, with a Tmax at 332 °C. This relates to the decomposition of the hard segments of the nanofibrous PU shell, as this degradation temperature is similar to other reported PU-based materials [63, 64]. Indeed, the hard segments of PU are thermally less stable than the soft segments [65]. A second peak can be observed in the DTG curve with a maximum at 420 °C, which relates to the decomposition of the soft segments of the nanofibrous PU shell and the PA6 core

yarn. The combined decomposition of both components results in a decrease of the Tmax in comparison to the PA6 core yarn. The addition of CHX does not affect the moisture resistivity of the PU CNYs, while a slight shift in the Tmax,1 can be observed. Also at higher temperatures, a different decomposition behavior can be observed. This suggests that the CHX molecules are interacting with the PU polymer chains, which alters their decomposition.

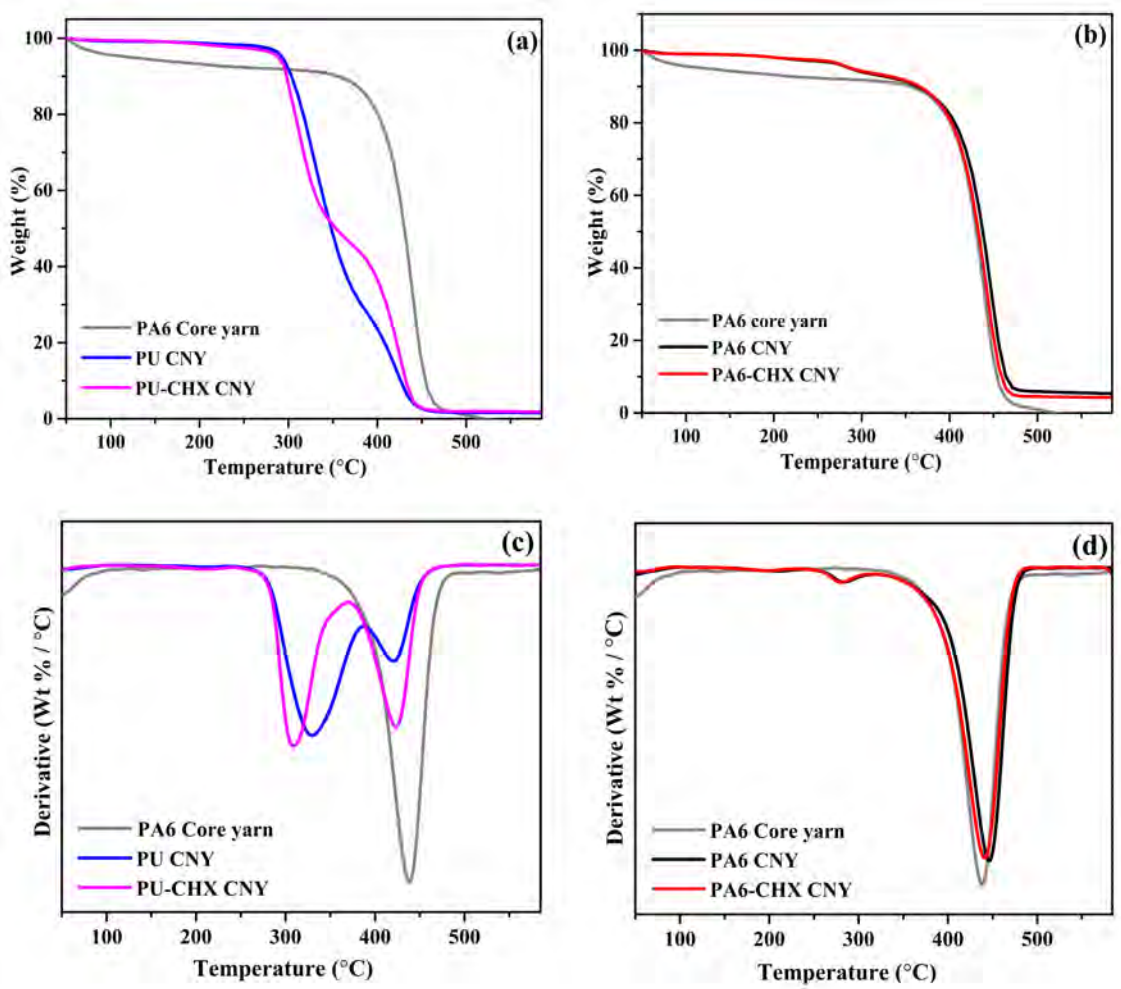

Figure 3.4: *(a, b) TGA thermograms of core, PU- and PA6-based CNYs, and (c, d) DTG thermograms of core, PU- and PA6-based CNYs.*

For the PA6 CNYs, an initial moisture resistivity is observed that is similar to the PU CNYs. This suggests that the nanofibrous nature of the PA6-based shell improves the moisture resistivity of the material, as PA6-based materials are typically sensitive to moisture (see also the previous paragraph). This is in line with the typically observed hydrophobic nature of nanofibrous mats, which originates from the entrapped air in the pores of the nanofibers [66]. In between 250 and 300 °C, a small weight loss can be observed, which could be related to the incorporated sulfuric acid-based components. The main single-step decomposition process of the PA6 CNYs is very similar to the decomposition of the PA6 core yarn, as it is made of the same material. The PA6 CNYs have slightly higher Tmax, which could be related to the interactions between the core and the shell of the CNYs. The addition of CHX results in a slight shift in the Tmax, which suggests that the CHX molecules interact in a different way with the PA6 than the PU polymer

chains. The abovementioned results clearly show that all fabricated CNYs are thermally stable until at least 250 °C, which is definitely sufficient for in vivo use as surgical sutures.

3.1.5 Antibacterial assay

The antibacterial activity of PU-CHX, PA6-CHX, and pristine PU and PA6 CNYs were tested by agar diffusion tests, as it is a commonly used technique to evaluate the antibacterial properties of sutures. As mentioned before, Gram-positive bacteria (*S. aureus*) and Gram-negative bacteria (*E. coli*) were used, as these bacterial strains are two major sources of SSIs. Fig. 3.5 displays the agar plates on which three CNYs are placed in the vertical direction per condition, as described in detail in section 2.4.9. It is clear that the PU- and PA6-based CNYs are not showing any antibacterial activity, as both *S. aureus* and *E. coli* are growing onto the material. For the PU-CHX samples, both bacterial strains can still be found on the surface of the CNYs, indicating that these yarns do not have any observable antibacterial activity. The PA6-CHX CNYs, however, are showing a clear antibacterial effect, as the growth of the microorganisms is clearly inhibited. A clear inhibition zone of 9±0.7 mm and 4±0.2 mm can be observed for *S. aureus* and *E. coli*, respectively. The fact that PA6-CHX CNYs have better antibacterial properties than the PU-CHX CNYs relates well with the amount of incorporated CHX as evaluated by HPLC in section 3.2. However, it contradicts the observations of the MTT assay, which is most likely caused by the difference in the CHX diffusion in the culture medium and the agar.

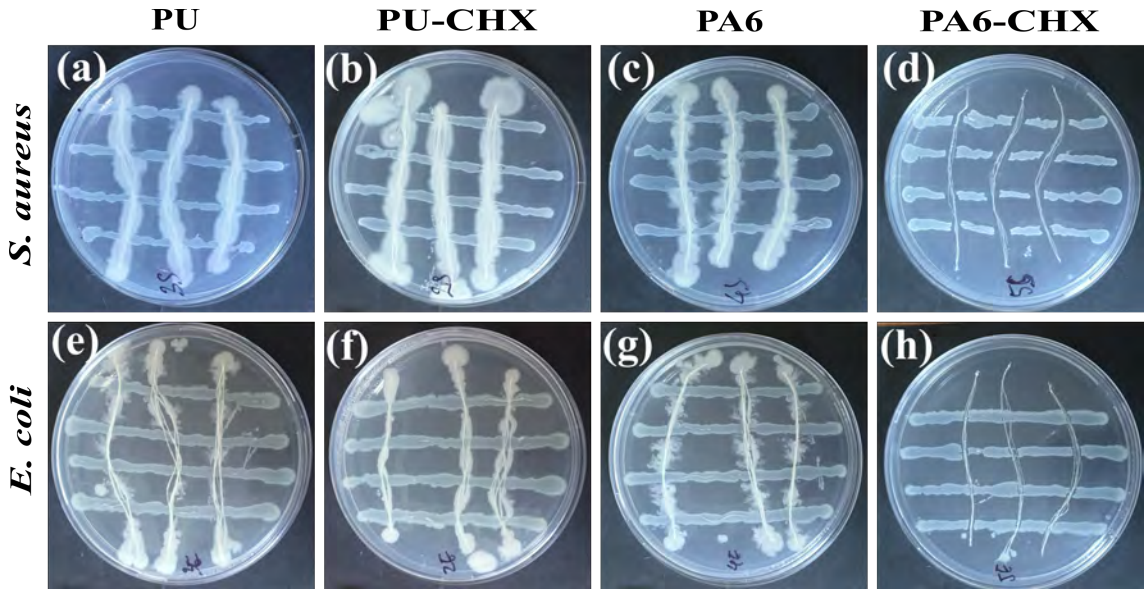

Figure 3.5: *Agar plates containing three CNYs to assess the zone of inhibition for S. aureus ((a,b),(c,d)) and E. coli ((e,f),(g,h)).*

3.1.6 Cytocompatibility of CNYs

In addition to the physico-chemical, mechanical thermal characterization, and antibacterial tests, also the cytocompatibility of the CNYs was examined by a MTT assay. Fig. 3.6 shows the cell viability of the pristine and CHX-containing CNYs in comparison to the control. Fig. 3.6 shows that the pristine PA6 and PU CNYs exhibit higher cell viability

than the control, indicating their good biocompatibility. After the addition of the CHX, the cell viability in the CNY-derived culture medium dropped below 70% for the PU-based material, which is considered the limit to still regard the material as cytocompatible. This could be expected, as both materials are typically considered as biocompatible. Apparently, the amount of leached-out CHX is too high for the PU-CHX CNYs, which results in a decrease in cell viability for this condition, as CHX can be cytotoxic above a certain threshold [67]. For the PA6-CHX CNYs, a statistically non-significant decrease in cell viability is observed, and the absorbance in the MTT assay is similar to the control, suggesting that these samples are biocompatible. The fact that the PA6-CHX CNYs contain a higher amount of CHX than the PU-CHX CNYs (Fig. 3.2c) also suggests that the characteristics of the resulting nanofibrous sheath can influence the CHX release kinetics.

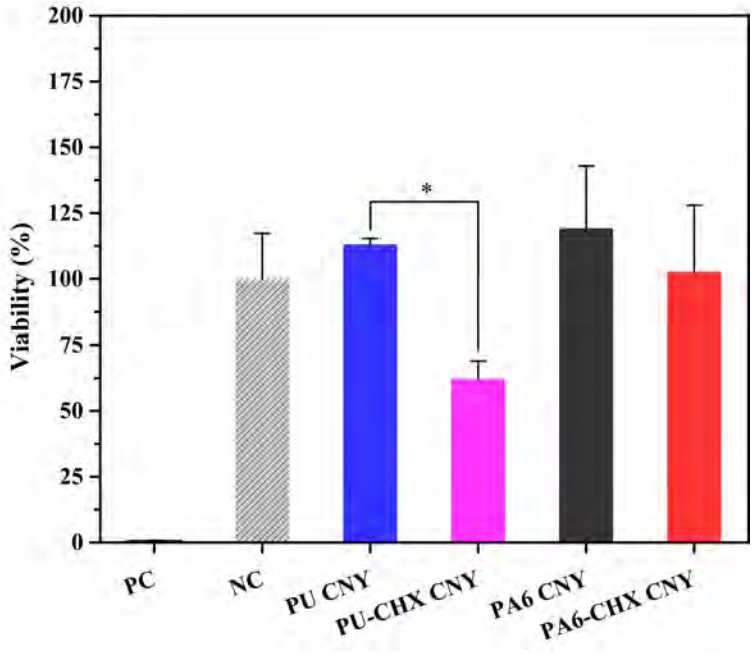

Figure 3.6: *Cell viability of the pristine and CHX-containing CNYs in comparison to the control. (*) indicates the statistically significant difference between the pristine and the CHX-containing PU CNYs as calculated with a unpaired t-test ($p < 0.05$).*

As such, it can be concluded that the PA6-CHX CNYs have antibacterial properties, are biocompatible and have superior mechanical characteristics, which makes them interesting for suture applications. Additionally, these results show that it is not necessary to observe significant changes in ATR-FTIR and XPS spectra after CHX addition to obtain a significant antibacterial effect, which is similar to what was observed for benzalkonium chloride-containing dental cement [49].

3.2 Continuous fabrication of functional braided PLA core PCL-PLA sheath CNYs

This sub-chapter 3.2 presents a method to fabricate functional braided CNYs for surgical sutures. Pristine and functional CNYs were produced using collectorless AC electrospinning, then braided to improve mechanical properties. Biocompatible PCL and PLA blends were used, with CHX and TRC as antibacterial agents. A PLA core was coated with the electrospun fibrous sheath, creating the composite yarn. The study examines morphology, physicochemical properties, mechanical strength, thermal stability, antibacterial activity, and cytotoxicity of the braided CNYs.

3.2.1 Spinnability and morphology of PLA/PCL-PLA–based braided CNYs

The pristine PCL-PLA, PCL-PLA-CHX, and PCL-PLA-TRC solutions were employed to fabricate the CNYs. The PCL-PLA solution initially failed to produce a steady fibrous plume due to poor AC spinnability. However, the addition of 0.5 wt% NaCl significantly improved its AC spinnability, resulting in the formation of a steady fibrous plume. Consequently, the PCL-PLA fibrous plume was coated onto the running PLA core yarn (30 m/min), thereby forming the desired core (PLA) - sheath (PCL- PLA) CNY. Comparatively, PCL-PLA-TRC exhibited a denser fibrous plume, followed by PCL-PLA-CHX and pristine PCL-PLA solutions. This observation indicates that drug-loaded solutions exhibited better AC spinnability without the addition of NaCl.

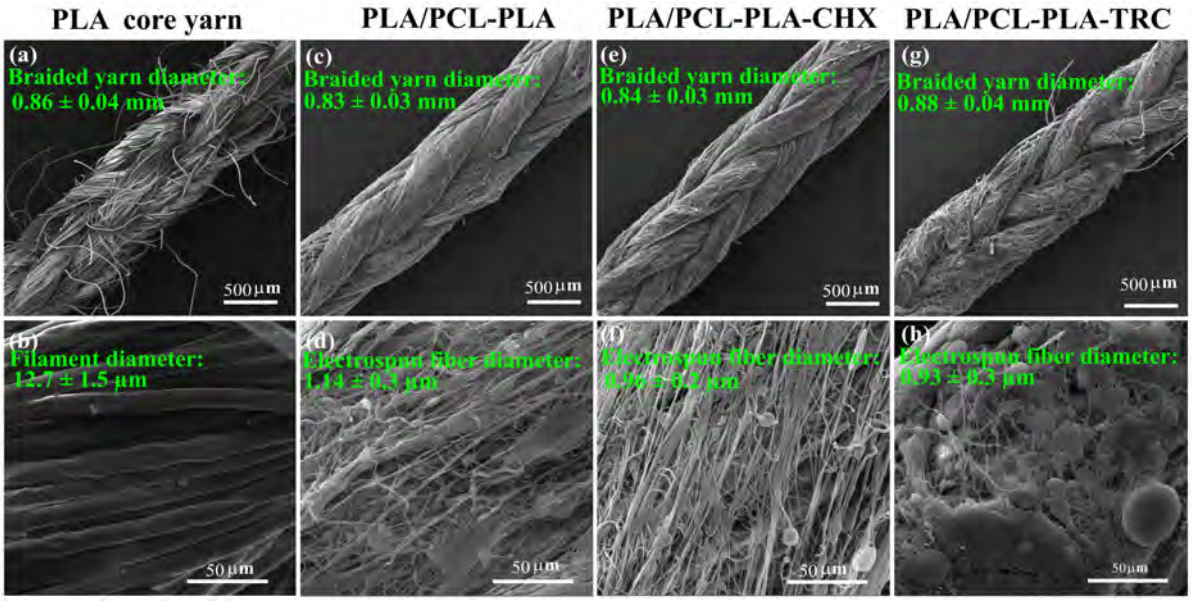

Figure 3.7: *SEM images of the braided PLA core yarn (a, and b), and various braided CNYs at different magnifications (c-h).*

The morphology of various braided CNYs and PLA core yarn was examined by SEM and is depicted in Fig. 3.7a-h. The SEM images illustrate the uniform electrospun deposition on the PLA core yarn. For each sample, 9 CNYs were utilized to create braided CNY. Throughout the braiding process, the maximum tension in the CNY was

maintained at 32 cN, facilitated by the custom-built yarn carrier, ensuring a smooth and efficient braiding process. SEM images of various braided CNYs indicate that the nanofibrous sheath layer remained undamaged and did not peel off from the CNY during or after braiding. Higher-resolution SEM images revealed clusters of beads on the string-like fibrous structure for PLA/PCL-PLA-TRC. Conversely, spindles and beads were observed on the fibrous surfaces of PLA/PCL-PLA and PLA/PCL-PLA-CHX.

3.2.2 Linear density of PLA/PCL-PLA–based braided CNYs

The gravimetric method was used to analyze as-fabricated CNY's linear density and theoretical linear density of electrospun fibrous sheath (Fig. 3.8a and b). The linear density of braided PLA core filament yarn is 2371 dtex. The pristine PLA/PCL-PLA braided CNY was 2595 dtex, in which 224 dtex (8.4 %) is covered by the nanofibrous envelope, and the remaining 2371 dtex (91.6 %) is core yarn. For the CHX and TRC loaded braided CNYs, the linear density was 2670 and 3070 dtex, in which 299 dtex (11.2 %) and 699 dtex (22.8 %) of nanofibers are covered on the core yarn 2371 (88.8 %) dtex and 2371 (77.2 %) dtex, respectively.

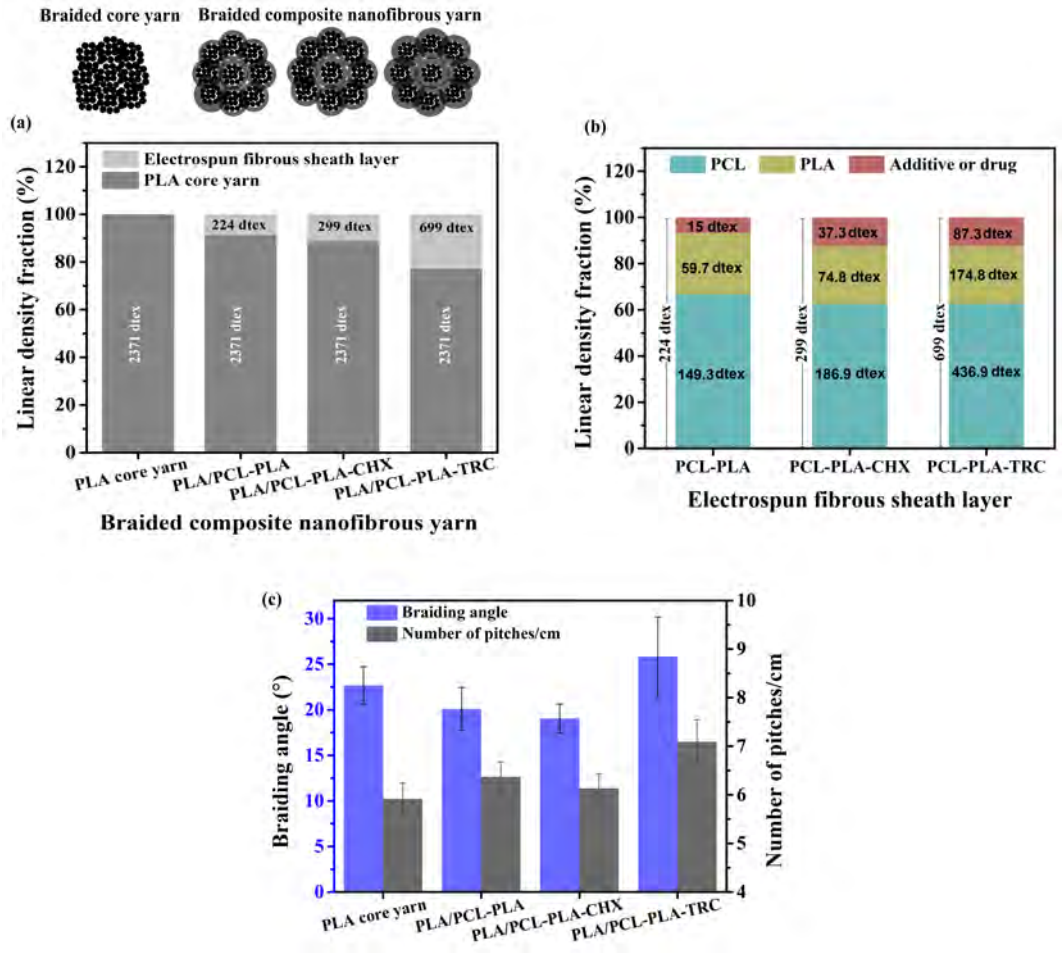

Figure 3.8: *Linear density of as-braided yarns (a), theoretical linear density of fibrous sheath layer (b), and (c) braiding angle and number of pitches/cm of as-fabricated yarns.*

The observed difference in the linear density of the electrospun fibrous sheath among the as-fabricated yarns is attributed to the spinnability of the spinning solutions, which

affects electrospun fiber productivity. The higher diameter, braiding angle (Fig. 3.8c), and number of pitches/cm (Fig. 3.8c) observed in the braided PLA/PCL-PLA-TRC yarn results from its higher linear density (Fig. 3.8a and b). Compared to the braided core yarn, the slight reduction in diameter observed in the braided pristine and CHX-loaded yarn is attributed to the nanofiber coating process and additional twisting during composite yarn fabrication, which tightened the CNY structure. Conversely, the multistranded structure and fraying of the PLA core yarn resulted in a larger diameter. Variations in braiding tension and compression also influence the diameter of the as-fabricated braided yarn, with the core yarn experiencing less compression during braiding. Additionally, the braiding angle and the number of pitches/cm impact the diameter by affecting yarn distribution and compression during the braiding process.

3.2.3 Chemical properties

The functional group analysis of various braided yarns was examined by FTIR (Fig. 3.9). For PLA, peaks at 2997 and 2954 cm^{-1} corresponded to asymmetric and symmetric CH stretching vibrations, respectively. Additionally, bands at 1748, 1453, 1383, 1358, 1128, and 1043 cm^{-1} were attributed to C=O stretching, CH3 bending, CH-asymmetric, symmetric deformation, C-O stretching, and OH bending, respectively [68].

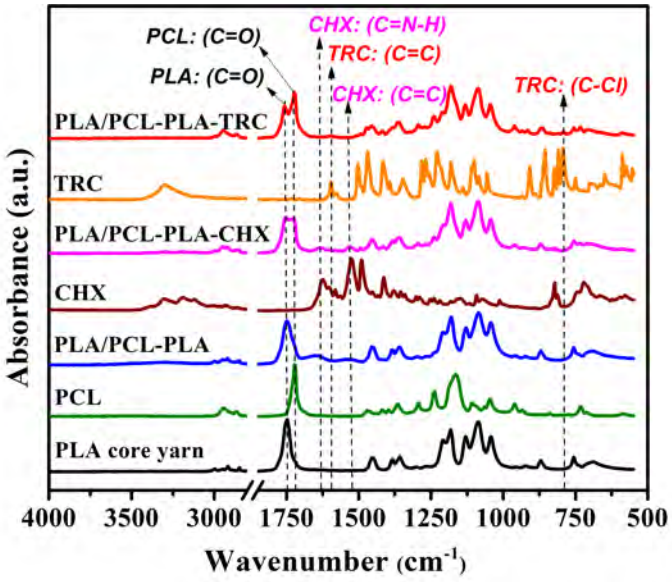

Figure 3.9: *FT-IR spectra of pristine and drug-loaded PLA/PCL-PLA braided CNYs.*

Concerning PCL, peaks at 2919 and 2851 cm^{-1} were assigned to asymmetric and symmetric CH2 stretching while, bands at 1722, 1294, 1238, and 1180 cm^{-1} were associated with C=O stretching, C-O & C-C stretching in the crystalline phase, and C-O asymmetric and symmetric stretching, respectively [38]. As expected, all the characteristic peaks of PLA and PCL were recognized in PLA/PCL-PLA braided CNY with changes in the intensity and wavenumber of the spectra [68]. CHX exhibited peaks at 1632 cm^{-1} (C=N-H stretching) and 1531/1493 cm^{-1} (aromatic C=C stretching) [69], while TRC showed characteristic peaks at 1597, 1508, and 1472 cm^{-1}, indicating C=C stretching. Moreover, the presence of C-Cl stretching was confirmed by the peak at 791 cm^{-1} [70]. The FTIR spectra of braided CNYs confirmed the presence of characteristic peaks from both PLA and PCL. In drug-loaded braided CNYs, the FTIR analysis confirmed the

presence of characteristic peaks corresponding to both the polymers and the drugs (CHX or TRC). In the case of PLA/PCL-PLA-TRC, the intensity of the C=O peak related to PCL was observed to be higher than that of PLA. This observation coincided with the respective linear densities, as shown in Fig. 3.8b, with PCL constituting 436.9 dtex and PLA comprising 174.8 dtex of the electrospun fibrous sheath.

3.2.4 Thermogravimetric analysis of as-fabricated yarns

The thermal stability was determined using thermogravimetric analysis, and the corresponding thermograms are depicted in (Fig 3.10a and b). For better visualization of the degradation process, the first derivative of the thermogram (DTG) is also presented in Fig. 3.10b. All fabricated samples showed thermal stability up to 270 °C. The braided PLA core yarn's maximum degradation temperature (Tmax) was observed at 344 °C with a single-step degradation. In comparison, PLA/PCL-PLA, PLA/PCL-PLA-CHX, and PLA/PCL-PLA-TRC exhibited two-step degradation. The first (Tmax1) and second (Tmax2) degradation temperatures of PLA/PCL-PLA were located at 332 and 361 °C, corresponding to PLA and PCL, respectively [68]. For PLA/PCL-PLA-CHX and PLA/PCL-PLA-TRC, Tmax1 was observed at 334 and 336 °C (corresponding to PLA). Meanwhile, Tmax2 was observed at 368 and 376 °C (related to PCL), respectively. The variations in Tmax1 and Tmax2 of pristine and drug-loaded samples clearly indicate the incorporation of CHX or TRC in the resultant braided yarns. Moreover, from Fig. 3.8b, and Fig. 3.10, it is evident that the Tmax2 peak intensity corresponding to PCL degradation increased as the linear density of the fibrous envelope increased (from 224 to 299 and 699 dtex). This is due to a 2.5 times higher amount of PCL (5 wt %) than PLA (2 wt %) in the fibrous envelope (Fig. 3.8b). TGA analysis further confirmed the presence of polymers and drugs in the braided CNYs.

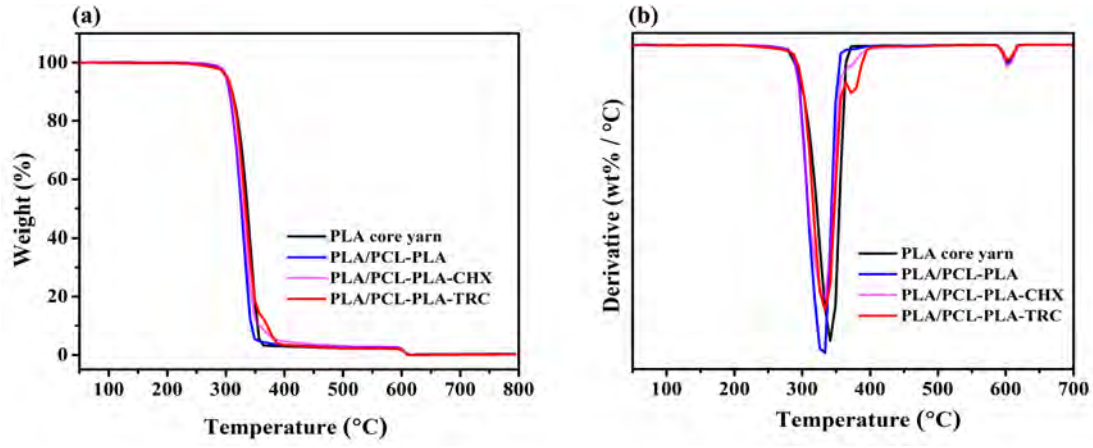

Figure 3.10: *(a) TGA thermogram, and (b) DTG thermogram of braided CNYs.*

3.2.5 Mechanical properties of PLA/PCL-PLA–based braided CNYs

The mechanical properties of the braided CNYs were evaluated in terms of maximum breaking force and extension (Fig. 3.11). Comparing the PLA braided core yarn with the braided CNYs revealed no significant difference in maximum breaking force ($p > 0.05$). This indicates that the PLA core yarn consistently maintains maximum breaking force, regardless of the linear density of its fibrous sheath layer,braiding angle, and number of

pitches/cm. However, the PLA/PCL-PCL-TRC exhibited significantly greater extension compared ($p < 0.05$) to the other yarns, likely due to the higher linear density of its nanofibrous sheath layer (Fig.3.8a and b).This enhanced extension is likely influenced by the higher braiding angle and pitches per centimeter observed in the PLA/PCL-PLA-TRC, resulting from the increased linear density of its nanofibrous sheath layer. Additionally, the higher PCL content in the fibrous sheath contributes to its greater elasticity, as PCL inherently possesses greater elasticity. As previously mentioned, in terms of mechanical properties, the PLA microfilament core layer contributes to the overall tensile breaking force while the electrospun sheath, braiding angle and number of pitches/cm contribute to the extension, particularly in the case of PLA/PCL-PLA-TRC.

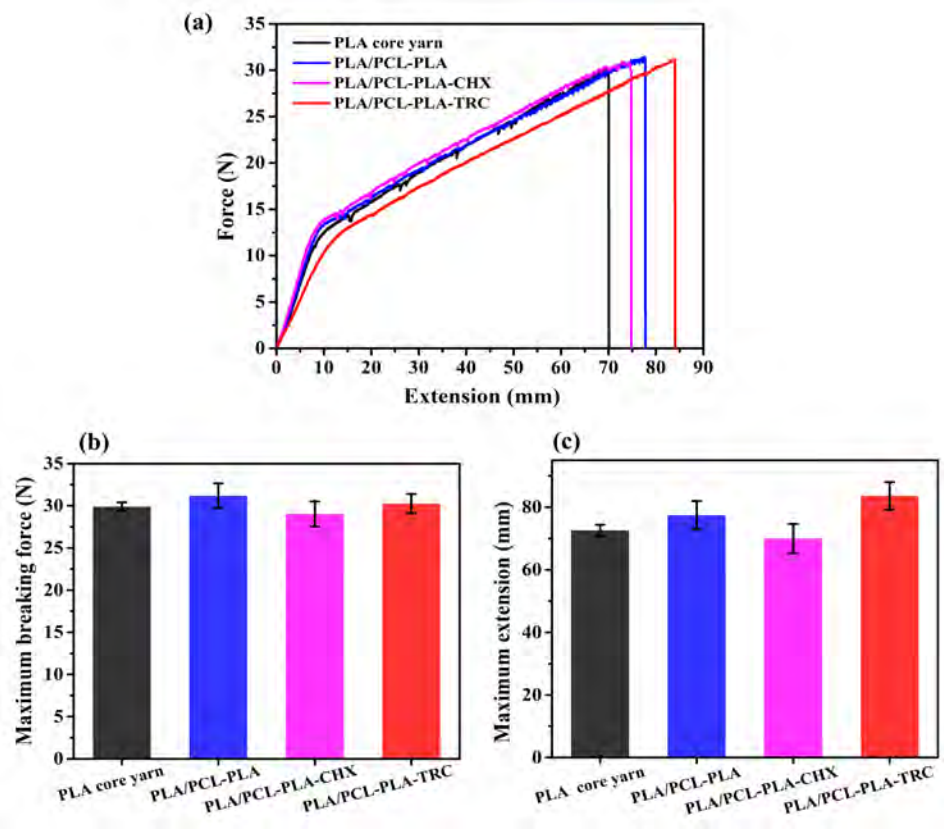

Figure 3.11: *Mechanical properties of pristine and functional PLA/PCL-PLA braided CNYs. (a) force-extension curve, (b) maximum breaking force, and (c) extension of pristine and functional PLA/PCL-PLA braided CNYs.*

3.2.6 Antibacterial efficiency and cytocompatibility of PLA/PCL-PLA–based braided CNYs

The antibacterial activity of as-fabricated materials was analyzed by agar diffusion test, and results are presented in Fig. 3.12a. Both Gram-positive (*S. aureus*) and Gram-negative (*E. coli*) bacterial strains were selected, as these strains commonly contribute to healthcare-associated infections. CHX or TRC diffuses from the drug-loaded samples and subsequently inhibits bacterial growth, resulting in a zone of inhibition. A clear inhibition zone of 2.25 ± 0.8 mm and 2.3 ± 0.5 mm can be observed on PLA/PCL-PLA-CHX for S. aureus and E. coli, respectively. In the case of PLA/PCL-PLA-TRC, 9.6 ± 0.8 mm and 7.5 ± 1.7 mm were observed for *S. aureus* and *E. coli*, respectively. The higher inhibition

zone of TRC-loaded yarn could be attributed to a higher amount of TRC (524 µg) than CHX (224 µg) in the braided yarn (length: 6 cm) used (Fig. 3.21). In contrast, as expected, bacterial growth (no inhibition zone) can be seen on pristine PLA/PCL-PLA, indicating that this braided yarn does not have antibacterial activity.

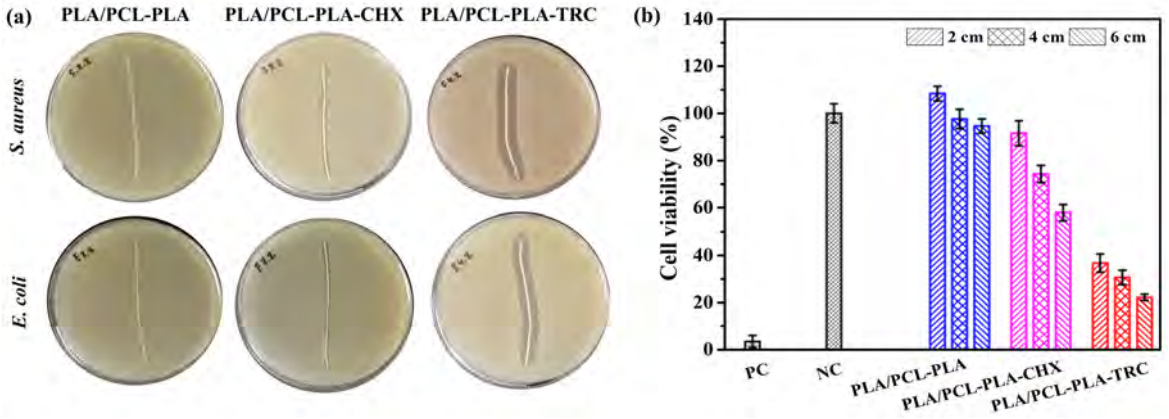

Figure 3.12: *(a) Antibacterial efficiency of PLA/PCL-PLA–based braided CNYs against S. aureus and E. coli. and (b) Cell viability as a function of various lengths of PLA/PCL-PLA–based braided CNYs.*

The antibacterial effect of drug-loaded materials must be balanced with the safety of eukaryotic cells, as they also require antibacterial protection. Therefore, the cytocompatibility of as-fabricated samples was examined by MTT assay with respect to their length (Fig.3.12b). The drug-free PLA/PCL-PLA showed higher cell viability than the drug-loaded samples, showing good biocompatibility. The increased metabolic activity in the 2 cm PLA/PCL-PLA yarn, compared to the 4 and 6 cm lengths, may be due to NaCl additive within the PCL-PLA nanofibrous sheath, known for its osmotic effect[71]. Approximately 30 µg of NaCl could have leached from the 2 cm yarn into the culture media, triggering osmotic pressure and resulting in higher metabolic activity than the longer lengths (Fig.3.12b and Fig. 3.22). PLA/PCL-PLA yarns of 4 and 6 cm lengths showed a slight reduction in metabolic activity, attributed to slightly higher NaCl leaching (60 and 90 µg, respectively (Fig.3.12b and Fig. 3.22). With the exception of the 6 cm length PLA/PCL-PLA-CHX, the 2 and 4 cm lengths exhibited cytocompatibility. In contrast, PLA/PCL-PLA-TRC showed cytotoxicity regardless of their lengths, as their cell viability was less than 70 %. As the length of the drug-loaded sample increased, a significantly higher amount of drug could have eluted into the cell media, consequently leading to decreased cell viability (Fig. 3.12b and Fig. 3.22).

It was reported that cell viability was oppositely proportional to an above-certain CHX or TRC threshold concentration [67, 72]. However, strategies such as braiding a combination of pristine and drug-loaded CNYs can enhance the biocompatibility of drug-loaded samples. By positioning the drug-loaded CNY at the core of the braided yarn structure and surrounding it with pristine CNYs, a protective barrier is created, limiting direct contact between the drug and surrounding tissues and thus enhancing biocompatibility. These strategies offer promising avenues for balancing antibacterial efficacy and biocompatibility in drug-loaded braided yarns, rendering them suitable for various surgical applications.

3.3 Continuous fabrication of functional braided PLA core PCL sheath CNYs

This sub-chapter 3.3 discusses the fabrication of braided CNYs using PLA as the core yarn and PCL, PCL with CHX, and PCL with TRC as the electrospun sheath layers. The resultant braided CNYs were produced using advanced AC electrospinning and braiding technology. The study explores the morphology, physicochemical characteristics, mechanical properties, thermal degradation, antibacterial activity, and cytotoxicity of the fabricated braided CNYs.

3.3.1 Spinnability and morphology of PLA/PCL–based braided CNYs

Pristine PCL and PCL blended with either CHX or TRC were used to fabricate both pristine and antibacterial drug-loaded CNYs using AC electrospinning. The surface topography of the various braided CNYs was evaluated using SEM, as depicted in Fig. 3.13.

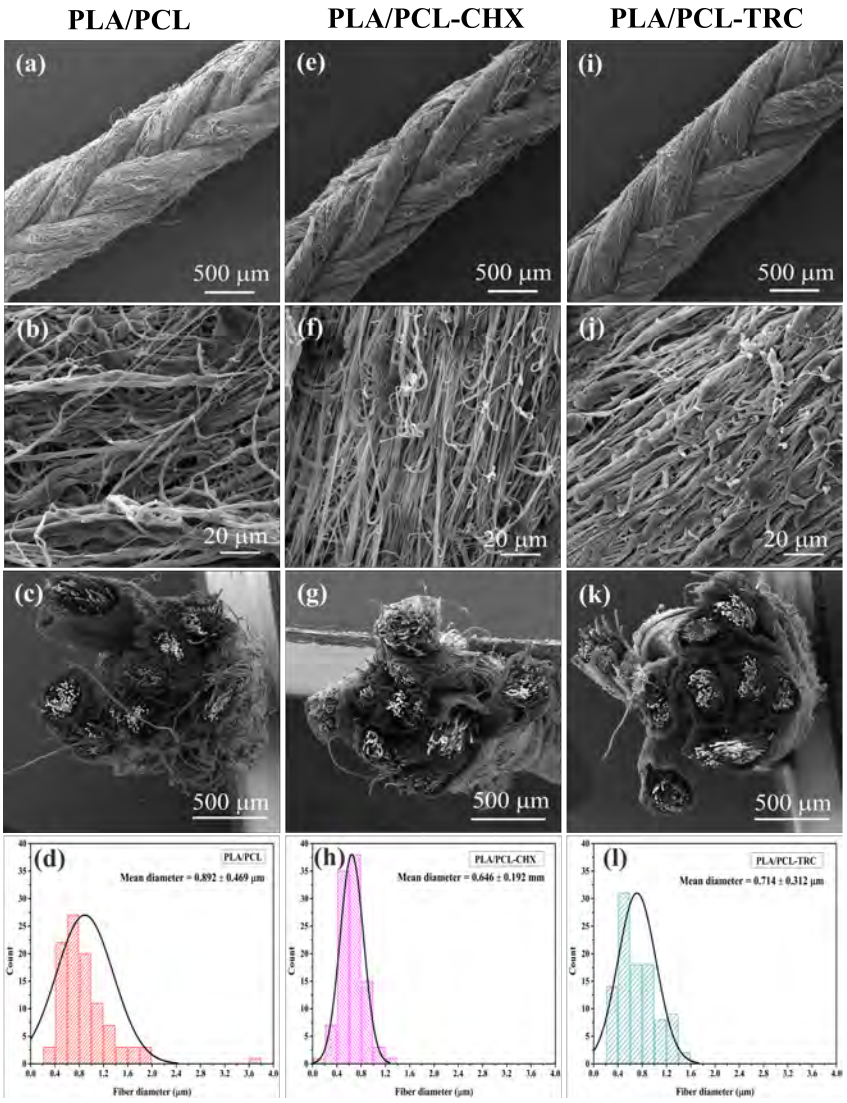

Figure 3.13: *SEM images and fiber diameter distribution of various braided CNYs. PLA/PCL (a-c) with fiber diameter distribution (d), PLA/PCL-CHX (e-g) with distribution (h), and PLA/PCL-TRC (i-k) with distribution (l).*

Fig. 3.13 clearly shows that the electrospun nanofibers of PCL, PCL-CHX, and PCL-TRC were completely wound around the PLA core yarn. This is attributed to the ability of the PCL, PCL-CHX, and PCL-TRC solutions to form a continuous, thicker fibrous plume that adheres to the running core yarn, resulting in the desired core-sheath nanofiber structure. A beaded nanofibrous morphology was observed in the PLA/PCL and PLA/PCL-TRC samples, with average fiber diameters of (0.892 ± 0.469) μm and (0.714 ± 0.312) μm, respectively. In contrast, the PLA/PCL-CHX samples consisted of smooth, electrospun fibers with a comparatively aligned fibrous morphology and an average fiber diameter of (0.646 ± 0.192) μm. Previous studies have reported that the addition of CHX to the pristine PCL solution results in lower viscosity and increased conductivity, which may explain the reduced fiber diameter in the PLA/PCL-CHX samples compared to the PLA/PCL or PLA/PCL-TRC samples [73]. Furthermore, during and after the braiding process, the nanofibrous envelope remained intact and did not peel off from the core yarn. The average diameters of the braided PLA/PCL, PLA/PCL-CHX, and PLA/PCL-TRC yarns were 1.01 ± 0.04 mm, 0.97 ± 0.04 mm, and 1.02 ± 0.02 mm, respectively.

3.3.2 Linear density of PLA/PCL–based braided CNYs

The linear density of PLA/PCL-based braided CNYs were calculated using a gravimetric method. The results are shown in Fig. 3.14a and b. The linear density of the PLA core braided yarn was determined to be 2371 dtex. For the braided PLA/PCL yarn, the linear density was 3778 dtex, with 1407 dtex (37%) contributed by the nanofibrous envelope and the remaining 2371 dtex (63%) by the core yarn.

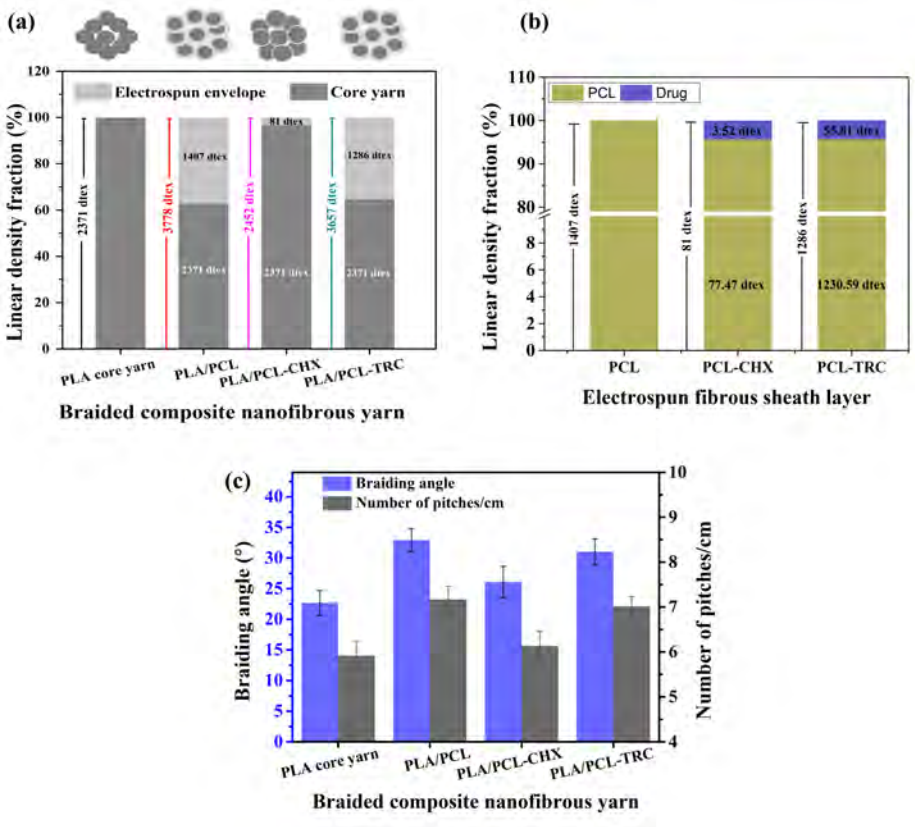

Figure 3.14: *Linear density of braided yarns (a), theoretical linear density of fibrous sheath (b), and braiding angle with number of pitches per cm (c).*

The linear density of the PLA/PCL-CHX braided composite yarn was 2452 dtex, of which 81 dtex (3%) was attributed to the nanofibrous envelope, and 2371 dtex (97%) to the core yarn. In the case of the PLA/PCL-TRC braided composite yarn, the linear density was 3657 dtex, with the nanofibrous envelope contributing 1286 dtex (35%) and the core yarn 2371 dtex (65%). Despite maintaining constant technological parameters across all samples during the fabrication process (refer to Table 2.2 on page 8), the CHX-loaded PLA/PCL yarn exhibited a lower linear density (Fig. 3.14a). This reduction can likely be attributed to the decreased AC spinnability of the CHX-loaded solution, which is associated with the increased conductivity of the polymeric solution due to the addition of CHX, as discussed in the previous section. On the other hand, the TRC-loaded samples demonstrated a higher linear density compared to the CHX-loaded ones. This increase in linear density for the TRC-loaded samples may be due to higher nanofiber productivity or, more specifically, better spinnability of the solution with the addition of TRC.

Similar to PLA/PCL-PLA based braided CNYs (Fig. 3.8 on page 25), the linear density of the nanofibrous sheath influences the diameter, braiding angle, and number of pitches/cm of the PLA/PCL-based braided CNYs (Fig. 3.14c). The braided PLA/PCL yarn exhibited a higher diameter, braiding angle, and number of pitches/cm, followed by the PLA/PCL-TRC and PLA/PCL-CHX CNYs, aligning with the observed linear density trend (Fig. 3.14a - c).

3.3.3 Chemical analysis of PLA/PCL–based braided CNYs

In order to confirm the presence of CHX and TRC in the antibacterial PLA/PCL braided CNYs, the elemental concentrations were determined using SEM-EDS.

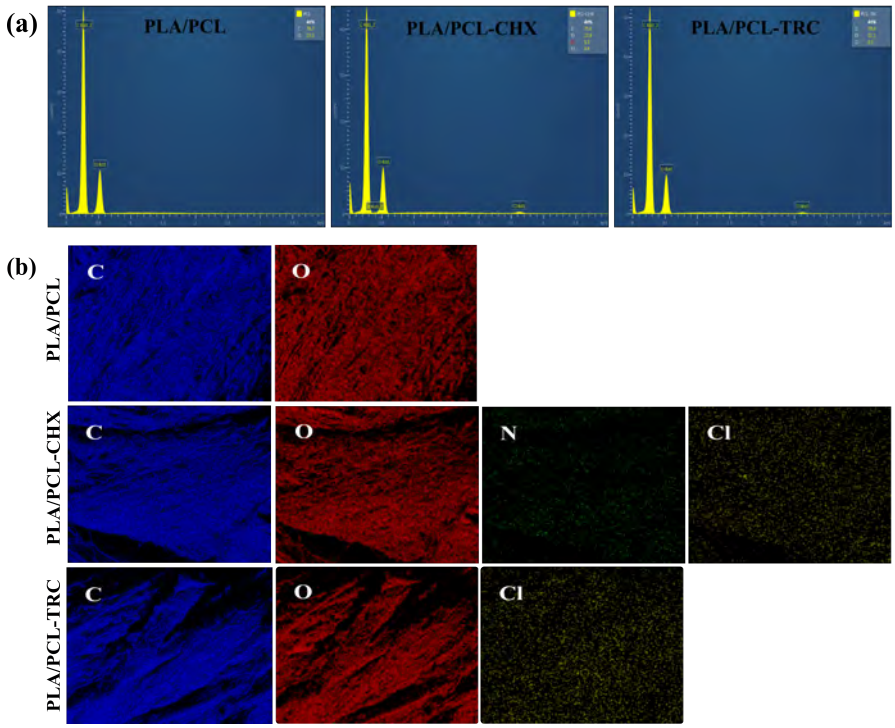

Figure 3.15: *EDS spectrum and elemental composition. EDS spectrums of PLA/PCL, PLA/PCL-CHX and PLA/PCL-TRC braided CNYs (a), and (b) elemental mapping images of resultant yarns (carbon (C), oxygen (O), nitrogen (N), and chlorine (Cl) elements).*

The SEM-EDS results for PLA/PCL, PLA/PCL-CHX, and PLA/PCL-TRC braided yarns were presented in Fig. 3.15a. As expected, the pristine PLA/PCL braided yarn showed only carbon and oxygen elements. For the CHX-loaded PLA/PCL yarn, in addition to carbon and oxygen, nitrogen and chlorine were detected, indicating the presence of CHX molecules on the surface (within the nanofibrous envelope). Similarly, for the TRC-loaded PLA/PCL yarn, chlorine was observed along with carbon and oxygen, confirming the presence of TRC molecules on the surface (within the nanofibrous envelope). The elemental mapping of the CHX and TRC-loaded PLA/PCL yarns clearly showed that CHX or TRC molecules were homogeneously distributed on the surface Fig. 3.15b.

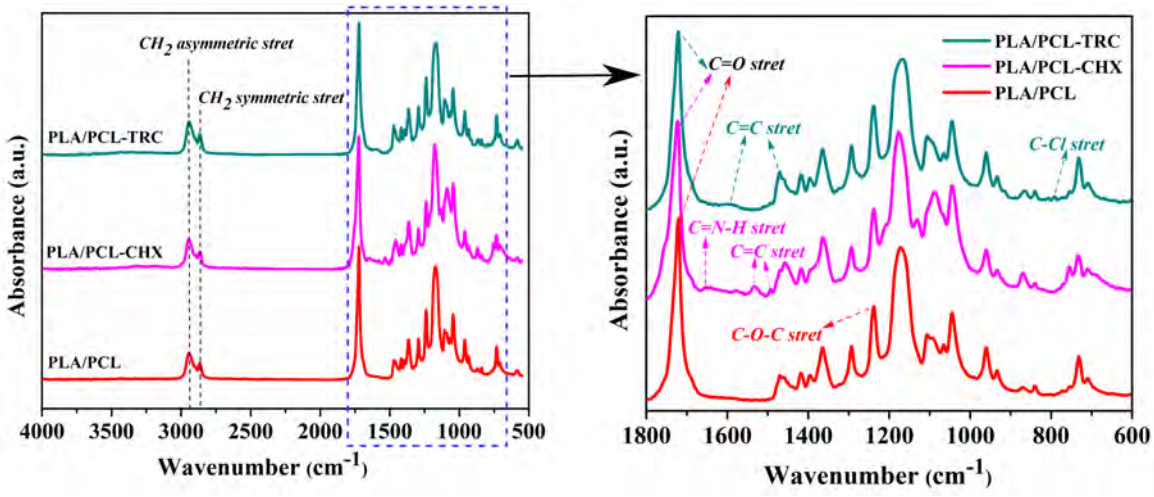

Figure 3.16: *FTIR spectrum of PLA/PLC, PLA/PCL-CHX and PLA/PCL-TRC braided CNYs (a), and corresponding magnified spectra (b).*

Furthermore, the functional group analysis of pristine PLA/PCL, PLA/PCL-CHX, and PLA/PCL-TRC braided CNYs was conducted using FTIR spectroscopy (Fig. 3.16). For PCL, characteristic bands corresponding to CH_2 asymmetric stretching at 2944 cm^{-1} and symmetric stretching at 2865 cm^{-1} were observed. The ester carbonyl group (C=O) peak appeared at 1726 cm^{-1}. The peak at 1238 cm^{-1} was attributed to C-O-C stretching, while the peak at 1177 cm^{-1} corresponded to C-O stretching [38]. In the CHX-loaded PLA/PCL samples, the characteristic peak of CHX at 1637 cm^{-1} was assigned to C=N-H stretching vibration. Additionally, peaks at 1532 cm^{-1} and 1491 cm^{-1} were attributed to aromatic C=C stretching vibrations [69]. For the TRC-loaded PLA/PCL samples, characteristic peaks in the 1610 – 1582 cm^{-1} and 1500 – 1400 cm^{-1} regions, corresponding to skeletal vibrations involving C-C stretching within the benzene ring, were observed at 1598, 1511, and 1471 cm^{-1}) [74]. Additionally, the presence of C–Cl stretching was confirmed by a peak at 791 cm^{-1}. The FTIR spectra of the PLA/PCL, PLA/PCL-CHX, and PLA/PCL-TRC braided yarns confirmed all the major characteristic peaks of PCL, CHX, and TRC. Hence, from both the FTIR and EDS analyses, it is evident that CHX and TRC were present on the nanofibrous envelope.

3.3.4 Thermal properties of PLA/PCL–based braided CNYs

The thermal degradation process of the PLA core yarn and PLA/PCL–based braided CNYs were evaluated using TGA and DTGA. The TGA and DTGA thermograms are shown in Fig. 3.17a and b. The PLA core yarn exhibits a single-step degradation process

and remains stable up to approximately 270 °C. The maximum degradation temperature (T_{max}) of PLA is observed at 344 °C. It is reported that, under a nitrogen atmosphere, PLA undergoes intramolecular transesterification, decomposing into acetaldehyde, carbon dioxide, carbon monoxide, water, and methane. At higher temperatures, lactide becomes the predominant degradation product [75].

The PLA/PCL and PLA/PCL-TRC samples are thermally stable up to approximately 270 °C, whereas PLA/PCL-CHX is stable up to around 150 °C. The PLA/PCL-based braided composite nanofibrous yarns exhibit two degradation steps with T_{max} at 325 °C and 379 °C, corresponding to the degradation of PLA and PCL chains, respectively. The degradation products of PCL include 5-hexanoic acid, carbon dioxide, carbon monoxide, and ε-caprolactone [75]. For PLA/PCL-CHX, the two-step degradation occurs at T_{max} of 295 °C and 372 °C, while for PLA/PCL-TRC, it occurs at 341 °C and 400 °C. The lower degradation temperatures in PLA/PCL-CHX, compared to PLA/PCL, are attributed to the incorporation of CHX, which also introduces a new degradation peak at 661 °C [76]. In contrast, the PLA/PCL-TRC sample shows higher degradation temperatures than PLA/PCL, indicating a successful incorporation of TRC and an effect on the thermal stability of the yarn.

These TGA and DTGA results are consistent with the linear density analysis. The linear density of PLA is highest in PLA/PCL-CHX, followed by PLA/PCL-TRC and PLA/PCL. Similarly, the DTGA results show that the intensity of the pristine PLA's thermogram is highest, followed by PLA/PCL-CHX, PLA/PCL-TRC, and PLA/PCL, reflecting the relative thermal stability and composition of the samples.

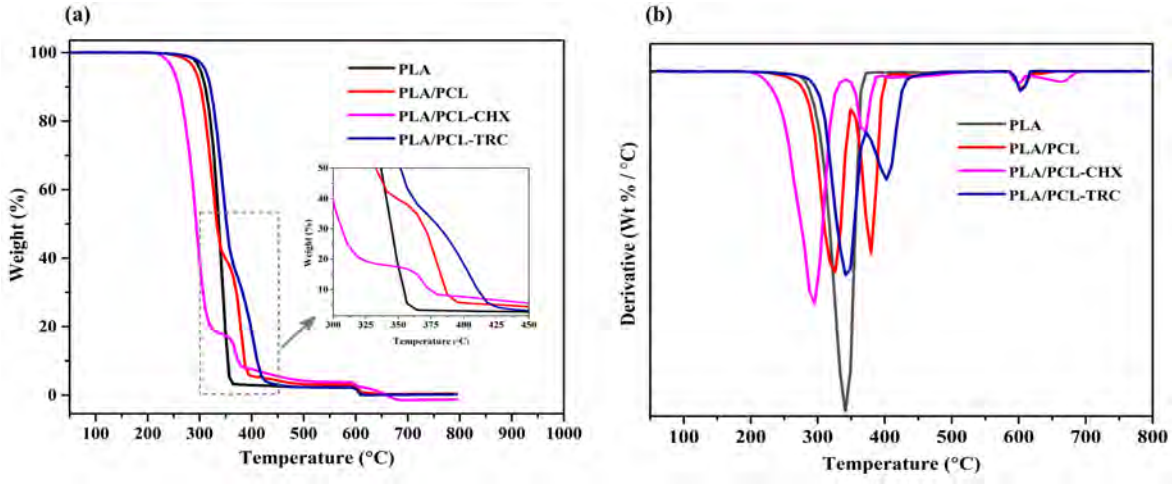

Figure 3.17: *(a) TGA thermogram, and (b) DTG thermogram of braided CNYs.*

3.3.5 Mechanical properties of PLA/PCL–based braided CNYs

In addition to the physicochemical properties, the mechanical properties of the braided yarns were analyzed, as these are crucial for their application as surgical sutures. The force-extension curve of the PLA core yarn, as shown in Fig. 3.18a, exhibits a zigzag or non-linear pattern. This behavior is attributed to the composition of the naked PLA core yarn, which consists of microfilaments. During stretching, some microfilaments may break

individually, causing fluctuations in the force-extension curve [77]. In contrast, the PLA core yarn covered with electrospun PCL, PCL-CHX, or PCL-TRC nanofibers displayed smooth force-extension curves without such fluctuations.

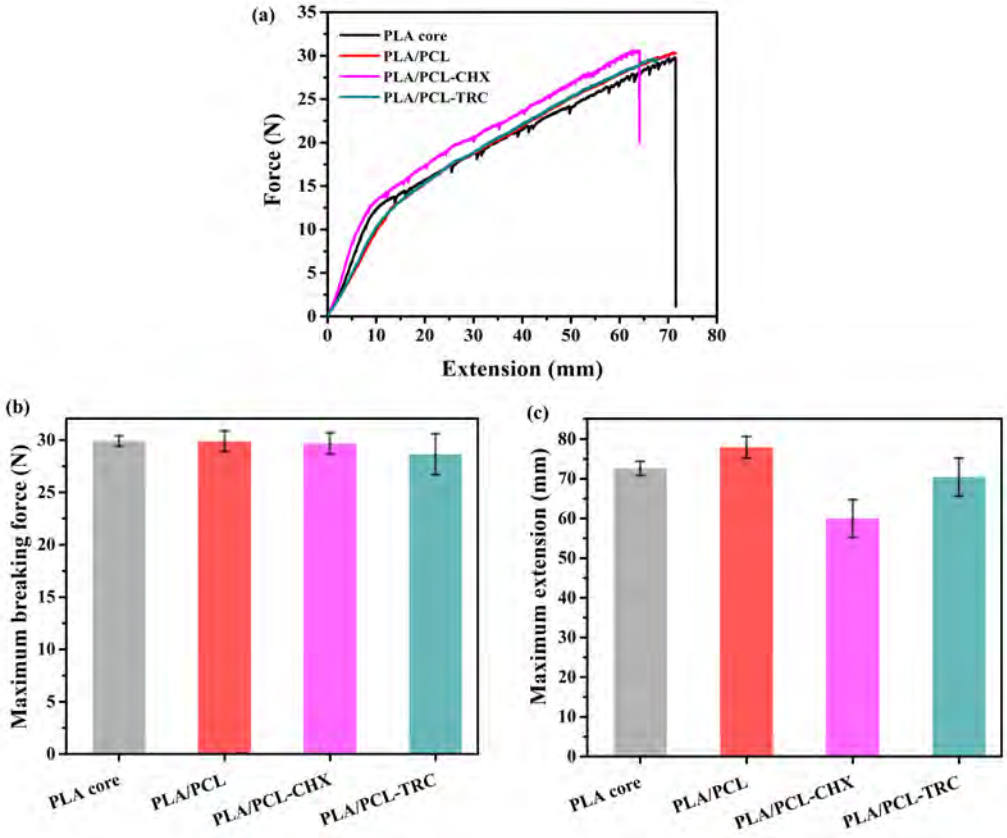

Figure 3.18: *Mechanical properties of pristine and functional PLA/PCL braided CNYs. (a) force-extension curve, (b) maximum breaking force, and (c) maximum extension of pristine and functional PLA/PCL braided CNYs.*

The maximum breaking force did not significantly differ among the braided core PLA yarn and the PLA/PCL-based braided CNYs, as illustrated in Fig. 3.18b. This observation indicates that the PLA core yarn provides the principal tensile strength, irrespective of the linear density of the fibrous sheath layer, braiding angle, or number of pitches/cm.However, a significant difference in extension was observed in the PLA/PCL-CHX braided CNY compared to the PLA/PCL and PLA/PCL-TRC samples, as seen in Fig. 3.18c. The reduced extension in the PLA/PCL-CHX braided CNY can be attributed to its lower linear density, reduced braiding angle, and fewer pitches per centimeter. The CHX-loaded sample's lower linear density suggests a more compact structure with less flexibility, while the modified braiding parameters may decrease the overall extensibility of the yarn.

Overall, the PLA microfilament core layer primarily contributes to the tensile breaking force, providing consistent strength across different yarn compositions. In contrast, the electrospun sheath, braiding angle, and number of pitches per centimeter predominantly affect the extension characteristics. All the fabricated braided yarns demonstrated a tensile strength of approximately 29 N, indicating that they possess adequate mechanical properties for potential use as surgical sutures.

3.3.6 Abrasion test of PLA/PCL–based braided CNYs

The abrasion tests were conducted as described in sub-chapter 2.4.8 on page 12, with the results presented in terms of morphological changes. As depicted in Fig. 3.19, the nanofibrous envelope of the braided PLA/PCL and PLA/PCL-TRC CNYs generally remains intact and was neither significantly damaged nor peeled off after various abrasion analyses. However, in the case of PLA/PCL-CHX samples, slight damage to the fibrous sheath was observed. This damage is primarily due to the lower linear density of the electrospun fibrous sheath layer. Additionally, specific interactions between the CHX molecules and the polymer matrix could potentially weaken the adhesion between the nanofibrous sheath and the core yarn. Nevertheless, this damage is relatively minor and does not significantly compromise the overall structural integrity of the braided CNYs. Despite minor damage in some cases, the preservation of the nanofibrous envelope can be attributed to the braided structure, which effectively maintains the integrity of the as-fabricated CNYs during the abrasion process and subsequent sewing operations.

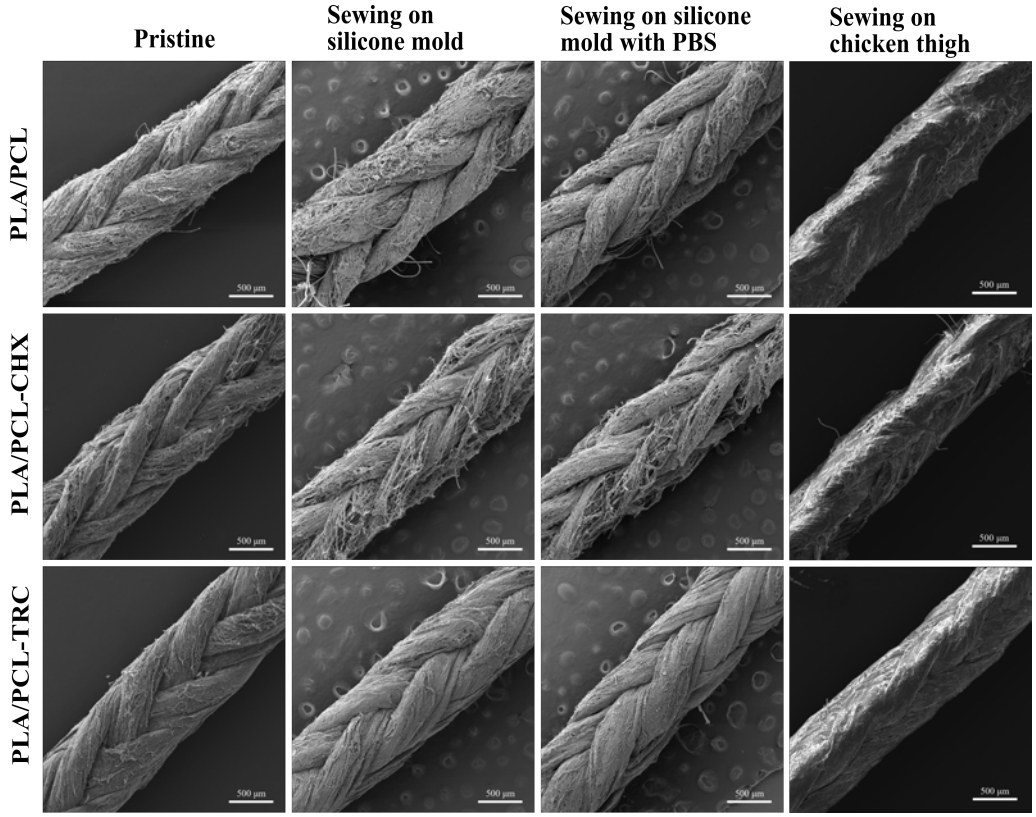

Figure 3.19: *SEM images of resultant yarns after various abrasion analysis (sewing on silicone mold with and without PBS, and sewing on chicken thigh) (Scale bar is 500 µm).*

3.3.7 Antimicrobial activity and cytotoxicity of PLA/PCL–based braided CNYs

The antibacterial activity of pristine PLA/PCL, as well as CHX- and TRC-loaded PLA/PCL braided CNYs, was tested using agar diffusion assays. As expected, the pristine PLA/PCL braided yarn showed no antibacterial activity, as evidenced by the visible growth of both *S. aureus* and *E. coli* in Fig. 3.20a. In contrast, CHX- and TRC-loaded PLA/PCL

braided yarns exhibited clear antibacterial effects, demonstrated by the inhibition of microorganism growth. Specifically, the inhibition zones for PLA/PCL-CHX were 6 ± 0.8 mm for *S. aureus* and 2.7 ± 0.9 mm for *E. coli*. For PLA/PCL-TRC, the inhibition zones measured 21 ± 0.4 mm for *S. aureus* and 7.33 ± 0.4 mm for *E. coli*.

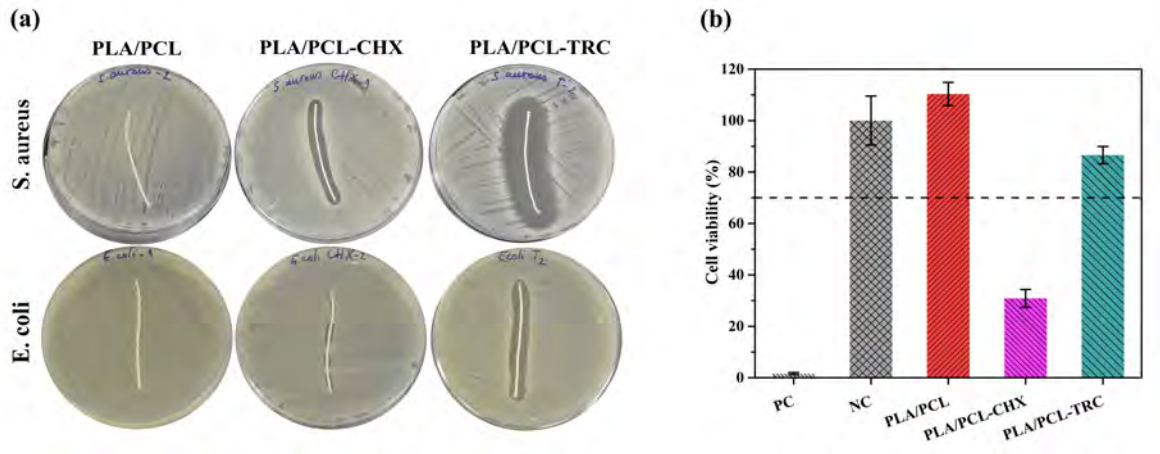

Figure 3.20: *(a) Antibacterial activity and (b) cytotoxicity analysis of PLA/PCL–based braided CNYs.*

In addition to examining physicochemical, mechanical, abrasion, and antibacterial properties, the cytocompatibility of the PLA/PCL-based CNYs was evaluated using the MTT assay. As shown in Fig. 3.20b, the cell viability of pristine and drug-loaded yarns was compared to a control. The results indicated that the pristine and TRC-loaded yarns exhibited higher cell viability than the CHX-loaded yarns, suggesting good biocompatibility. Reducing the CHX concentration in the spinning solution may be necessary to balance the antibacterial efficacy with cell safety.

Overall, this sub–chapter 3.3 analyzed PLA/PCL-based braided CNYs, focusing on their potential biomedical applications as surgical sutures. TRC-loaded braided PLA/PCL CNY demonstrated superior antibacterial activity and better cytocompatibility, indicating their promise for infection control. All variants maintained robust structural integrity during abrasion tests, and their tensile strength was sufficient for surgical use. Chemical and thermal analyses confirmed the effective incorporation and distribution of antimicrobial agents, enhancing the yarns' functional properties. Overall, these findings suggest that PLA/PCL-based braided CNYs, especially with TRC, offer significant potential as advanced, durable, and biocompatible materials for medical applications, particularly in the development of effective, infection-resistant surgical sutures.

3.4 Appendix

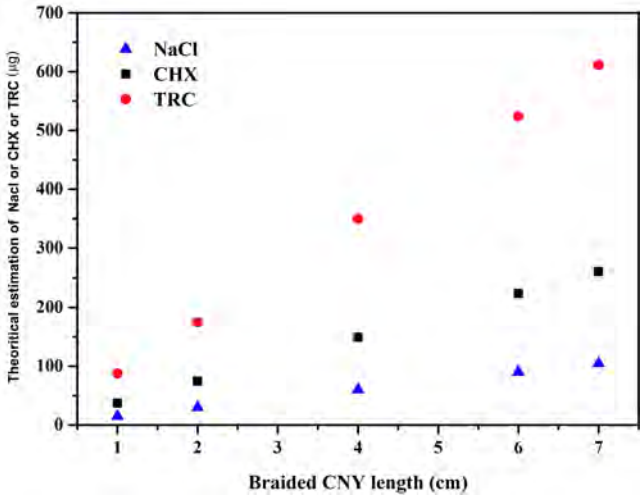

Figure 3.21: *Theoretical estimation of NaCl or CHX or TRC in the braided PLA/PCL-PLA CNY.*

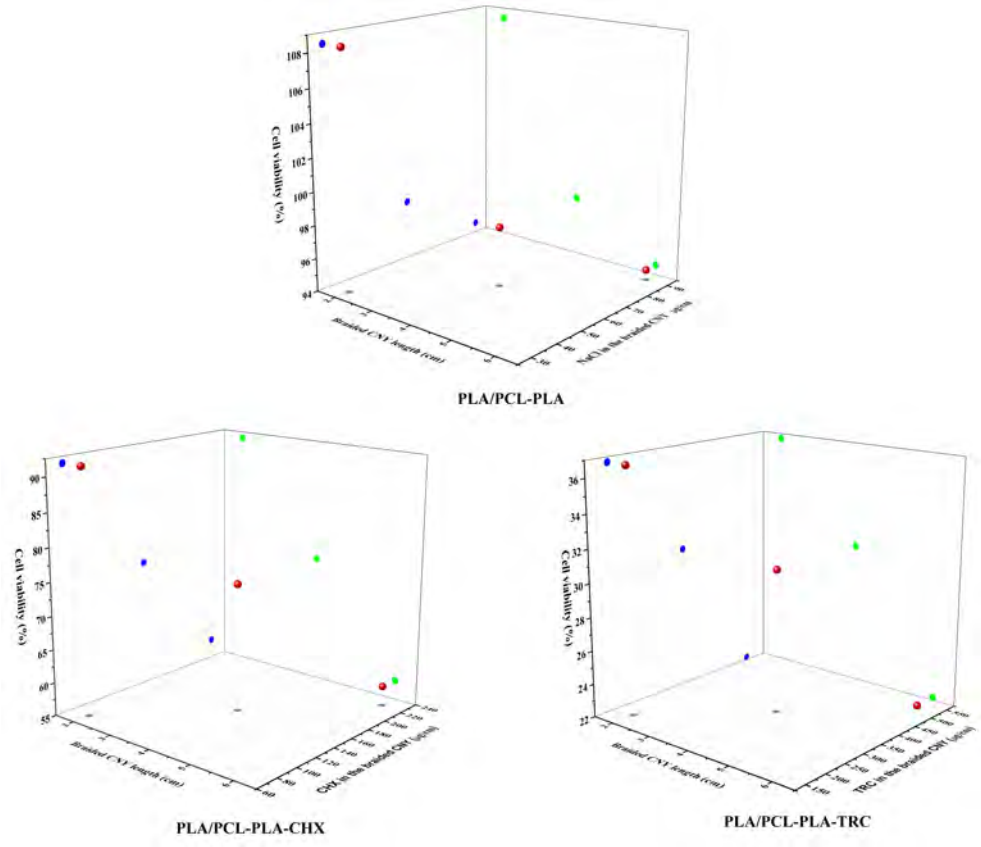

Figure 3.22: *Relationship between the braided CNY length, theoretical estimation of NaCl or CHX or TRC in braided CNY, and cell viability.*

4. Evaluation of the results and new findings

This dissertation introduces braided CNYs as an innovative approach for smart surgical sutures. While surgical sutures remain a critical biomaterial in healthcare, there have been no groundbreaking advancements aimed at enhancing their multifunctionality or providing nanoscale fibrillar support for cellular activities. The electrospun sheath layer facilitates the simultaneous incorporation of multiple functional components, such as antibacterial agents, anti-inflammatory substances, growth factors, and analgesics, thus accelerating the wound healing process. Meanwhile, the core yarn ensures the necessary mechanical properties. The development of these novel braided electrospun yarns represents a significant step forward in the field, offering potential improvements in the performance and therapeutic capabilities of sutures, thus paving the way for future innovations in wound healing and tissue regeneration. Additionally, the use of AC electrospinning and braiding technology supports the industrial-scale production of these yarns, presenting a significant advantage.

The research was conducted in three main parts:

❶ **Development of Pristine and Antibacterial PU– and PA6–based CNYs:**

- ❍ Pristine and CHX-loaded PU and PA6 CNYs were fabricated using AC electrospinning at the production rates of 20 m/min and 10 m/min, respectively.
- ❍ SEM confirmed the complete wrapping of the nanofibrous sheath around the PA6 core yarn.
- ❍ HPLC and FTIR spectroscopy verified the presence of CHX in the PU-CHX and PA6-CHX CNYs.
- ❍ The maximum breaking forces of 2.2 N for PU-based and 1.7 N for PA6-based CNYs were observed.
- ❍ TGA analysis confirmed thermal stability up to at least 250 °C for all CNYs
- ❍ MTT assays showed biocompatibility for PU, PA6, and PA6-CHX CNYs.
- ❍ Antibacterial tests revealed that PA6-CHX CNYs effectively inhibited bacterial growth, making them suitable as antibacterial surgical sutures.

❷ **Fabrication of Braided PLA/PCL-PLA–based CNYs:**

- ❍ Pristine and antibacterial CNYs, including PLA/PCL-PLA, PLA/PCL-PLA-CHX, and PLA/PCL-PLA-TRC, were successfully fabricated using AC electrospinning at a production rate of 30 m/min.
- ❍ These CNYs were braided at a production rate of 0.25 m/min without compromising the structural integrity of the electrospun sheath layer. SEM analysis confirmed their structural integrity.

- FTIR verified the presence of CHX or TRC in the braided CNYs.
- These braided CNYs exhibited a maximum breaking force of 29 N and thermal stability up to 270 °C.
- Cytotoxicity and antibacterial properties assessments indicated that the PLA/PCL-PLA-CHX was biocompatible and effective against bacteria, making it suitable for surgical suture applications.

❸ **Fabrication of Braided PLA/PCL–based CNYs:**

- The third experimental phase involved the production of pristine and CHX- or TRC-loaded PLA/PCL CNYs via AC electrospinning at a production rate of 12 m/min.
- The resultant CNYs were braided at a production rate of 0.25 m/min without compromising the structural integrity of the electrospun sheath layer. SEM analysis validated the successful fabrication of these braided yarns.
- FTIR confirmed the incorporation of CHX or TRC in the braided CNYs.
- These braided CNYs also showed a tensile breaking force of 29 N and thermal stability up to 270 °C.
- Cytotoxicity and antibacterial tests confirmed that PLA/PCL-TRC was biocompatible and effective against bacteria, making it a viable option for surgical sutures.

Overall, the study confirmed that the developed braided CNYs, using advanced AC electrospinning and braiding technologies, possess excellent breaking strength ($\geq$29 N) and high thermal stability ($\geq$270°C). The successful incorporation of antibacterial agents was verified through antibacterial efficiency tests and FTIR analysis. Cytotoxicity analysis demonstrated that CHX-loaded PA6 CNY, braided PLA/PCL-PLA CNY, and TRC-loaded PLA/PCL CNY could function as thermally stable, mechanically robust, biocompatible, and antibacterial surgical sutures.

4.0.1 Significant Outputs, Limitations, and Future Work

Significant Outputs

- The integration of AC electrospinning and braiding technologies enabled the creation of novel surgical sutures with enhanced mechanical properties, biocompatibility, and antibacterial efficacy.
- The electrospun sheath layer allows for loading multiple functional components, such as antibacterial agents, anti-inflammatory substances, growth factors, and analgesics, thereby accelerating the wound healing process.

- The study demonstrated an efficient, scalable production method for braided CNYs, suitable for industrial-scale manufacturing.
- The developed braided CNYs have potential applications beyond surgical sutures, including tissue engineering, filtration systems, wearable electronics, and sensors.

Limitations

- The study identified weak adhesion between the electrospun fibrous sheath and the core yarn, which needs improvement to enhance the mechanical integrity of the sutures (addressed partially by braiding technology).
- Although the electrospinning process was efficient, the braiding process had a relatively low production rate of 0.25 m/min, which could limit large-scale manufacturing.

Future work

- Future research will focus on balancing antibacterial effects with cytotoxicity by braiding a combination of pristine and drug-loaded CNYs to enhance biocompatibility.
- Knot-pull-out and suture creep tests will be analyzed to further evaluate the mechanical properties of the braided CNYs.
- Clinical trials will be conducted on these braided CNYs (in vivo) to assess their performance in real-world medical applications.
- Research will continue to explore new material combinations and fabrication techniques to optimize the performance and application scope of the CNYs.

This research establishes a strong foundation for the development of next-generation surgical sutures and other biomedical materials, promising significant advancements in medical treatments and beyond.

References

[1] James M Adovasio, Olga Soffer, and Bohuslav Klíma. Upper palaeolithic fibre technology: interlaced woven finds from pavlov i, czech republic, c. 26,000 years ago. *Antiquity*, 70(269):526–534, 1996.

[2] Chih-Chang Chu, J Anthony von Fraunhofer, and Howard P Greisler. *Wound closure biomaterials and devices*. CRC Press, 2018.

[3] William R Wagner, Shelly E Sakiyama-Elbert, Guigen Zhang, and Michael J Yaszemski. *Biomaterials science: an introduction to materials in medicine*. Academic Press, 2020.

[4] Sabu Thomas, Phil Coates, Ben Whiteside, Blessy Joseph, and Karthik Nair. *Advanced Technologies and Polymer Materials for Surgical Sutures*. Woodhead Publishing, 2022.

[5] Tuba Baygar, Nurdan Sarac, Aysel Ugur, and Inci Rana Karaca. Antimicrobial characteristics and biocompatibility of the surgical sutures coated with biosynthesized silver nanoparticles. *Bioorganic chemistry*, 86:254–258, 2019.

[6] Surgical sutures market, 2023. URL `https://www.marketsandmarkets.com/Market-Reports/surgical-sutures-market-18374832.html`.

[7] Daniele Massella, Monica Argenziano, Ada Ferri, Jinping Guan, Stéphane Giraud, Roberta Cavalli, Antonello A Barresi, and Fabien Salaün. Bio-functional textiles: Combining pharmaceutical nanocarriers with fibrous materials for innovative dermatological therapies. *Pharmaceutics*, 11(8):403, 2019.

[8] Shaohua Wu, Ting Dong, Yiran Li, Mingchao Sun, Ye Qi, Jiao Liu, Mitchell A Kuss, Shaojuan Chen, and Bin Duan. State-of-the-art review of advanced electrospun nanofiber yarn-based textiles for biomedical applications. *Applied Materials Today*, 27:101473, 2022.

[9] Christopher Igwe Idumah, Anthony Chidi Ezika, and Uzoma Ebenezer Enwerem. A review on biomolecular immobilization of polymeric textile biocomposites, bionanocomposites, and nano-biocomposites. *The Journal of The Textile Institute*, 113(9):2016–2032, 2022.

[10] Christopher Dennis, Swaminathan Sethu, Sunita Nayak, Loganathan Mohan, Yosry Morsi, and Geetha Manivasagam. Suture materials—current and emerging trends. *Journal of Biomedical Materials Research Part A*, 104(6):1544–1559, 2016.

[11] Mythili Tummalapalli, Sadiya Anjum, Shanti Kumari, and Bhuvanesh Gupta. Antimicrobial surgical sutures: Recent developments and strategies. *Polymer Reviews*, 56(4):607–630, 2016.

[12] Albina R Franco, Emanuel M Fernandes, Márcia T Rodrigues, Fernando J Rodrigues, Manuela E Gomes, Isabel B Leonor, David L Kaplan, and Rui L Reis. Antimicrobial coating of spider silk to prevent bacterial attachment on silk surgical sutures. *Acta biomaterialia*, 99:236–246, 2019.

[13] Hang Liu, Karen K Leonas, and Yiping Zhao. Antimicrobial properties and release profile of ampicillin from electrospun poly (εepsilon;-caprolactone) nanofiber yarns. *Journal of Engineered Fibers and Fabrics*, 5(4):155892501000500402, 2010.

[14] Shixuan Chen, Liangpeng Ge, Aubrey Mueller, Mark A Carlson, Matthew J Teusink, Franklin D Shuler, and Jingwei Xie. Twisting electrospun nanofiber fine strips into functional sutures for sustained co-delivery of gentamicin and silver. *Nanomedicine: Nanotechnology, Biology and Medicine*, 13(4):1435–1445, 2017.

[15] Kunal S Parikh, Revaz Omiadze, Aditya Josyula, Richard Shi, Nicole M Anders, Ping He, Youseph Yazdi, Peter J McDonnell, Laura M Ensign, and Justin Hanes. Ultra-thin, high strength, antibiotic-eluting sutures for prevention of ophthalmic infection. *Bioengineering & Translational Medicine*, 6(2):e10204, 2021.

[16] Muhammad Nadeem Shuakat and Tong Lin. Recent developments in electrospinning of nanofiber yarns. *Journal of nanoscience and nanotechnology*, 14(2):1389–1408, 2014.

[17] Magnus Kruse, Marc Greuel, Franziska Kreimendahl, Thomas Schneiders, Benedict Bauer, Thomas Gries, and Stefan Jockenhoevel. Electro-spun pla-peg-yarns for tissue engineering applications. *Biomedical Engineering/Biomedizinische Technik*, 63(3):231–243, 2018.

[18] CR Reshmi, Rosebin Babu, Shantikumar V Nair, and Deepthy Menon. Recent advances in electrospun nanofibrous polymeric yarns. *Electrospun Polymeric Nanofibers: Insight into Fabrication Techniques and Biomedical Applications*, pages 107–137, 2023.

[19] F Mokhtari, M Salehi, F Zamani, F Hajiani, F Zeighami, and M Latifi. Advances in electrospinning: The production and application of nanofibres and nanofibrous structures. *Textile Progress*, 48(3):119–219, 2016.

[20] Manikandan Sivan. *Studies on the spinnability and surface modification of polycaprolactone nanofibers produced by AC electrospinning*. Ph.d. thesis, Technical University of Liberec, 2022.

[21] Nakamwi Akombaetwa, Alick Bwanga, Pedzisai Anotida Makoni, and Bwalya A Witika. Applications of electrospun drug-eluting nanofibers in wound healing: Current and future perspectives. *Polymers*, 14(14):2931, 2022.

[22] Jiao Liu, Huiyuan Zhai, Yaning Sun, Shaohua Wu, and Shaojuan Chen. Developing high strength poly (l-lactic acid) nanofiber yarns for biomedical textile materials: A comparative study of novel nanofiber yarns and traditional microfiber yarns. *Materials Letters*, 300:130229, 2021.

[23] Rosebin Babu, John Joseph, Binulal N Sathy, Shantikumar V Nair, Praveen Kerala Varma, and Deepthy Menon. Design, development, and evaluation of an interwoven electrospun nanotextile vascular patch. *Macromolecular Materials and Engineering*, 306(11):2100359, 2021.

[24] Ailin Li, Liming Wang, and Xiaohong Qin. Manufacturing and application of electrospinning nanofiber yarn. *Electrospinning: Fundamentals, Methods, and Applications*, pages 45–69, 2024.

[25] Yuhang Wang, Zhi Wang, Hongyan Fu, Haoyi Li, Jing Tan, and Weimin Yang. Preparation and functional applications of electrospun yarns. *Functionalized Nanofibers*, pages 109–133, 2023.

[26] Jaroslav Beran, Jan Valtera, Martin Bilek, Josef Skrivanek, Ondrej Batka, David Lukas, Pavel Pokorny, Tomas Kalous, Julie SoukupovaOUKUPOVA, Eva Kostakova, et al. Method for producing polymeric nanofibers by electrospinning a polymer solution or melt, a spinning electrode for performing the method and a device for producing polymeric nanofibers equipped with at least one such spinning electrode, 2017.

[27] Jaroslav Beran, Jan Valtera, Martin Bilek, Ondrej Batka, Josef Skrivanek, Petr Zabka, Jiri Komarek, David Lukas, Pavel Pokorny, Eva Kuzelova-Kostakova, et al. Linear fibrous formation with a coating of polymeric nanofibers enveloping a supporting linear formation constituting a core, a method and a device for producing it, February 23 2021. US Patent 10,927,480.

[28] Jaroslav Beran, David Lukas, Pavel Pokorny, Tomas Kalous, and Jan Valtera. Method for producing polymeric nanofibres by electric or electrostatic spinning of a polymer solution or melt, a spinning electrode for the method, and a device for the production of polymeric nanofibres equipped with at least one such spinning electrode, October 26 2021. US Patent 11,155,934.

[29] Lubomir Kocis, Pavel Pokorny, David Lukas, Petr Mikes, Jiri Chvojka, Eva Kostakova, Jaroslav Beran, Martin Bilek, Jan Valtera, Evzen Amler, et al. Method for production of polymeric nanofibers by spinning of solution or melt of polymer in electric field, August 7 2018. US Patent 10,041,189.

[30] Pavel Pokorny, E Kostakova, Filip Sanetrnik, Petr Mikes, Jiri Chvojka, Tomas Kalous, Martin Bilek, Karel Pejchar, Jan Valtera, and David Lukas. Effective ac needleless and collectorless electrospinning for yarn production. *Physical Chemistry Chemical Physics*, 16(48):26816–26822, 2014.

[31] Siddharth Maheshwari and Hsueh-Chia Chang. Assembly of multi-stranded nanofiber threads through ac electrospinning. *Advanced Materials*, 21(3):349–354, 2009.

[32] M Sivan, D Madheswaran, S Hauzerova, V Novotny, V Hedvicakova, V Jencova, EK Kostakova, M Schindler, and D Lukas. Ac electrospinning: Impact of high voltage and solvent on the electrospinnability and productivity of polycaprolactone electrospun nanofibrous scaffolds. *Materials Today Chemistry*, 26:101025, 2022.

[33] Manikandan Sivan, Divyabharathi Madheswaran, Jan Valtera, Eva Kuzelova Kostakova, and David Lukas. Alternating current electrospinning: The impacts of various high-voltage signal shapes and frequencies on the spinnability and productivity of polycaprolactone nanofibers. *Materials & Design*, 213:110308, 2022.

[34] Jan Valtera, Tomas Kalous, Pavel Pokorny, Ondrej Batka, Martin Bilek, Jiri Chvojka, Petr Mikes, Eva Kuzelova Kostakova, Petr Zabka, Jana Ornstova, et al. Fabrication of dual-functional composite yarns with a nanofibrous envelope using high throughput ac needleless and collectorless electrospinning. *Scientific reports*, 9(1):1801, 2019.

[35] Tomas Kalous, Pavel Holec, Radek Jirkovec, David Lukas, and Jiri Chvojka. Improved spinnability of pa 6 solutions using ac electrospinning. *Materials Letters*, 283:128761, 2021.

[36] Radek Jirkovec, Tomas Kalous, and Jiri Chvojka. The modification of the wetting of polycaprolactone nanofibre layers via alternating current spinning. *Materials & Design*, 210:110096, 2021.

[37] Pavel Holec, Tomáš Kalous, Jan Vinter, Jakub Erben, Pavel Pokornỳ, Alžbeta Samková, Jiří Brožek, and Jiří Chvojka. The alternating current electrospinning of aliphatic polyamides solutions enhanced with sulfuric acid. *Journal of Industrial and Engineering Chemistry*, 2023.

[38] Manikandan Sivan, Divyabharathi Madheswaran, Mahtab Asadian, Pieter Cools, Monica Thukkaram, Pascal Van Der Voort, Rino Morent, Nathalie De Geyter, and David Lukas. Plasma treatment effects on bulk properties of polycaprolactone nanofibrous mats fabricated by uncommon ac electrospinning: A comparative study. *Surface and Coatings Technology*, 399:126203, 2020.

[39] Andrei Stanishevsky, W Anthony Brayer, Pavel Pokorny, Tomáš Kalous, and David Lukáš. Nanofibrous alumina structures fabricated using high-yield alternating current electrospinning. *Ceramics International*, 42(15):17154–17161, 2016.

[40] S Mahalingam, R Matharu, S Homer-Vanniasinkam, and M Edirisinghe. Current methodologies and approaches for the formation of core–sheath polymer fibers for biomedical applications. *Applied Physics Reviews*, 7(4), 2020.

[41] Petr Ryšánek, Marek Malỳ, Pavla Čapková, Martin Kormunda, Zdeňka Kolská, Milan Gryndler, Ondřej Novák, Lucie Hocelíková, Lukáš Bystrianskỳ, and Marcela Munzarová. Antibacterial modification of nylon-6 nanofibers: structure, properties and antibacterial activity. *Journal of Polymer Research*, 24:1–10, 2017.

[42] Alaa J Hassiba, Mohamed E El Zowalaty, Thomas J Webster, Aboubakr M Abdullah, Gheyath K Nasrallah, Khalil Abdelrazek Khalil, Adriaan S Luyt, and Ahmed A Elzatahry. Synthesis, characterization, and antimicrobial properties of novel double layer nanocomposite electrospun fibers for wound dressing applications. *International Journal of Nanomedicine*, pages 2205–2213, 2017.

[43] Liang Chen, Lev Bromberg, T Alan Hatton, and Gregory C Rutledge. Electrospun cellulose acetate fibers containing chlorhexidine as a bactericide. *Polymer*, 49(5):1266–1275, 2008.

[44] SJ Najafi, AA Gharehaghaji, and SM Etrati. Fabrication and characterization of elastic hollow nanofibrous pu yarn. *Materials & Design*, 99:328–334, 2016.

[45] Ali Bahadur, Muhammad Shoaib, Aamer Saeed, and Shahid Iqbal. Ft-ir spectroscopic and thermal study of waterborne polyurethane-acrylate leather coatings using tartaric acid as an ionomer. *e-Polymers*, 16(6):463–474, 2016.

[46] George Socrates. *Infrared and Raman characteristic group frequencies: tables and charts*. John Wiley & Sons, 2004.

[47] Renée Onnainty, Barbara Onida, Paulina Páez, Marcela Longhi, Antonello Barresi, and Gladys Granero. Targeted chitosan-based bionanocomposites for controlled oral mucosal delivery of chlorhexidine. *International journal of pharmaceutics*, 509(1-2):408–418, 2016.

[48] Pierre Pouponneau, Ophélie Perrey, Céline Brunon, Carol Grossiord, Nicolas Courtois, Vincent Salles, and Antoine Alves. Electrospun bioresorbable membrane eluting chlorhexidine for dental implants. *Polymers*, 12(1):66, 2020.

[49] Tamer Tüzüner, Zeynep A Güçlü, Andrew Hurt, Nichola J Coleman, and John W Nicholson. Release of antimicrobial compounds from a zinc oxide-chelate cement. *Journal of Oral Science*, 60(1):24–28, 2018.

[50] Siyuan Jiang, Yufei Liu, Xiaoyu Zou, Min He, Kai Zhang, Guomin Xu, and Shuhao Qin. Synthesis and application of new macromolecular hindered phenol antioxidants of polyamide 6. *Journal of Applied Polymer Science*, 138(40):51184, 2021.

[51] Shengming Zhang, Jingchun Zhang, Lian Tang, Jiapeng Huang, Yunhua Fang, Peng Ji, Chaosheng Wang, and Huaping Wang. A novel synthetic strategy for preparing polyamide 6 (pa6)-based polymer with transesterification. *Polymers*, 11(6):978, 2019.

[52] Hem Raj Pant, Madhab Prasad Bajgai, Chuan Yi, R Nirmala, Ki Taek Nam, Woo-il Baek, and Hak Yong Kim. Effect of successive electrospinning and the strength of hydrogen bond on the morphology of electrospun nylon-6 nanofibers. *Colloids and Surfaces A: Physicochemical and Engineering Aspects*, 370(1-3):87–94, 2010.

[53] Ki-Taek Nam, Hem Raj Pant, Jin-won Jeong, Bishweshwar Pant, Byeong-il Kim, and Hak-Yong Kim. Solvent degradation of nylon-6 and its effect on fiber morphology of electrospun mats. *Polymer degradation and stability*, 96(11):1984–1988, 2011.

[54] Ruiguang Li, Lin Ye, and Guangxian Li. Long-term hydrothermal aging behavior and aging mechanism of glass fibre reinforced polyamide 6 composites. *Journal of Macromolecular Science, Part B*, 57(2):67–82, 2018.

[55] Ronaldo P Parreño, Ying-Ling Liu, Arnel B Beltran, and Maricar B Carandang. Effect of a direct sulfonation reaction on the functional properties of thermally-crosslinked electrospun polybenzoxazine (pbz) nanofibers. *RSC advances*, 10(24):14198–14207, 2020.

[56] Rino Morent, Nathalie De Geyter, Christophe Leys, L Gengembre, and E Payen. Comparison between xps-and ftir-analysis of plasma-treated polypropylene film surfaces. *Surface and Interface Analysis: An International Journal devoted to the development and application of techniques for the analysis of surfaces, interfaces and thin films*, 40(3-4):597–600, 2008.

[57] Mihkel Viirsalu, Natalja Savest, Tiia Plamus, Viktoria Vassiljeva, and Andres Krumme. Novel method for producing electrospun composite nanofibre yarns. *Proceedings of the Estonian Academy of Sciences*, 67(2):169–174, 2018.

[58] Haitao Niu, Weimin Gao, Tong Lin, Xungai Wang, and Lingxue Kong. Composite yarns fabricated from continuous needleless electrospun nanofibers. *Polymer Engineering & Science*, 54(7):1495–1502, 2014.

[59] Bin Zhang, Xu Yan, Yuan Xu, Huai-Song Zhao, Miao Yu, and Yun-Ze Long. Measurement of adhesion of in situ electrospun nanofibers on different substrates by a direct pulling method. *Advances in Materials Science and Engineering*, pages 1–8, 2020.

[60] Chan-Hee Park, Chae-Hwa Kim, Leonard D Tijing, Do-Hee Lee, Mi-Hwa Yu, Hem Raj Pant, Yonjig Kim, and Cheol Sang Kim. Preparation and characterization of (polyurethane/nylon-6) nanofiber/(silicone) film composites via electrospinning and dip-coating. *Fibers and Polymers*, 13:339–345, 2012.

[61] I Carrascal, JA Casado, JA Polanco, and F Gutiérrez-Solana. Absorption and diffusion of humidity in fiberglass-reinforced polyamide. *Polymer composites*, 26(5):580–586, 2005.

[62] Lin Sang, Chuo Wang, Yingying Wang, and Wenbin Hou. Effects of hydrothermal aging on moisture absorption and property prediction of short carbon fiber reinforced polyamide 6 composites. *Composites Part B: Engineering*, 153:306–314, 2018.

[63] Xing-Yan Huang, Cornelis F de Hoop, Xiao-Peng Peng, Jiu-Long Xie, Jin-Qiu Qi, Yong-Ze Jiang, Hui Xiao, and Shuang-Xi Nie. Thermal stability analysis of polyurethane foams made from microwave liquefaction bio-polyols with and without solid residue. *BioResources*, 13(2):3346–3361, 2018.

[64] Xingxing Shi, Saihua Jiang, Jingyi Zhu, Guohui Li, and Xiangfang Peng. Establishment of a highly efficient flame-retardant system for rigid polyurethane foams based on bi-phase flame-retardant actions. *RSC advances*, 8(18):9985–9995, 2018.

[65] JM Cervantes-Uc, JI Moo Espinosa, JV Cauich-Rodríguez, A Avila-Ortega, H Vázquez-Torres, A Marcos-Fernández, and Julio San Román. Tga/ftir studies of segmented aliphatic polyurethanes and their nanocomposites prepared with commercial montmorillonites. *Polymer Degradation and Stability*, 94(10):1666–1677, 2009.

[66] Rouba Ghobeira, Charlot Philips, Len Liefooghe, Marieke Verdonck, Mahtab Asadian, Pieter Cools, Heidi Declercq, Winnok H De Vos, Nathalie De Geyter, and Rino Morent. Synergetic effect of electrospun pcl fiber size, orientation and plasma-modified surface chemistry on stem cell behavior. *Applied Surface Science*, 485:204–221, 2019.

[67] Jiankang Song, Stefan JA Remmers, Jinlong Shao, Eva Kolwijck, X Frank Walboomers, John A Jansen, Sander CG Leeuwenburgh, and Fang Yang. Antibacterial effects of electrospun chitosan/poly (ethylene oxide) nanofibrous membranes loaded with chlorhexidine and silver. *Nanomedicine: Nanotechnology, Biology and Medicine*, 12(5):1357–1364, 2016.

[68] Pongthep Prajongtat, Chakrit Sriprachuabwong, Ratchada Wongkanya, Decha Dechtrirat, Jutarat Sudchanham, Nirachawadee Srisamran, Winyoo Sangthong, Piyachat Chuysinuan, Adisorn Tuantranont, Supa Hannongbua, et al. Moisture-resistant electrospun polymer membranes for efficient and stable fully printable perovskite solar cells prepared in humid air. *ACS applied materials & interfaces*, 11(31):27677–27685, 2019.

[69] JG Fernandes, Daniela M Correia, Gabriela Botelho, Jorge Padrão, Fernando Dourado, Clarisse Ribeiro, Senentxu Lanceros-Méndez, and Vitor Sencadas. Phb-peo electrospun fiber membranes containing chlorhexidine for drug delivery applications. *Polymer Testing*, 34:64–71, 2014.

[70] Mehmet Orhan. Triclosan applications for biocidal functionalization of polyester and cotton surfaces. *Journal of Engineered Fibers and Fabrics*, 15:1558925020940104, 2020.

[71] Elton Stubblefield and Gerald C Mueller. Effects of sodium chloride concentration on growth, biochemical composition, and metabolism of hela cells. *Cancer Research*, 20(11):1646–1655, 1960.

[72] Luis J Del Valle, Roger Camps, Angélica Díaz, Lourdes Franco, Alfonso Rodríguez-Galán, and Jordi Puiggalí. Electrospinning of polylactide and polycaprolactone mixtures for preparation of materials with tunable drug release properties. *Journal of polymer research*, 18:1903–1917, 2011.

[73] Sivan Manikandan, Madheswaran Divyabharathi, K Tomas, P Pavel, and L David. Production of poly (ε-caprolactone) antimicrobial nanofibers by needleless alternating current electrospinning. *Materials Today: Proceedings*, 17:1100–1104, 2019.

[74] Asli Celebioglu and Tamer Uyar. Electrospinning of polymer-free nanofibers from cyclodextrin inclusion complexes. *Langmuir*, 27(10):6218–6226, 2011.

[75] Christian Vogel and Heinz W Siesler. Thermal degradation of poly (ε-caprolactone), poly (l-lactic acid) and their blends with poly (3-hydroxy-butyrate) studied by tga/ft-ir spectroscopy. In *Macromolecular symposia*, volume 265, pages 183–194. Wiley Online Library, 2008.

[76] Balasankar M Priyadarshini, Subramanian T Selvan, Karthikeyan Narayanan, and Amr S Fawzy. Characterization of chlorhexidine-loaded calcium-hydroxide microparticles as a potential dental pulp-capping material. *Bioengineering*, 4(3):59, 2017.

[77] Ziqi Gu, Haiyue Yin, Juan Wang, Linlin Ma, Yosry Morsi, and Xiumei Mo. Fabrication and characterization of tgf-β1-loaded electrospun poly (lactic-co-glycolic acid) core-sheath sutures. *Colloids and Surfaces B: Biointerfaces*, 161:331–338, 2018.

5. Research outputs

5.1 List of Publication

Three manuscripts as the first-author; h–index = 5; citations = 162, (WoS updated on 14/10/2024)

1. **Madheswaran D**, Sivan M, Hauzerova S, Kostakova E.K, Jencova V, Valter J, Behalek L, Mullerova J, Nguyen, NH, Capek, L. and Lukas D "*Continuous fabrication of braided composite nanofibrous surgical yarns using advanced AC electrospinning and braiding technology*". Composites Communications, 48:101932, 2024.
   Impact Factor (2023): 6.5 (Q1). Citations: 5.

2. **Madheswaran D**, Sivan, M., Valtera J, Kostakova EK, Egghe T, Asadian M, Novotny V, Nguye, NH, Sevcu A, Morent R, De Geyter N, and Lukas D "*Composite yarns with antibacterial nanofibrous sheaths produced by collectorless alternating–current electrospinning for suture applications*". Journal of Applied Polymer Science, 139(13): 51851, 2022. Impact Factor (2023): 2.7 (Q2). Citations: 11.

3. Sivan, M., **Madheswaran D**, Hauzerova S, Novotny V, Hedvicakova V, Jencova V, Kostakova EK, Schindler M. and Lukas D. "*AC electrospinning: impact of high voltage and solvent on the electrospinnability and productivity of polycaprolactone electrospun nanofibrous scaffolds*". Materials Today Chemistry, 26:101025, 2022.
   Impact Factor (2023): 6.7 (Q1). Citations: 46.

4. Sivan M, **Madheswaran D**, Valtera J, Kostakova EK, Lukas D, "*Alternating current electrospinning: The impacts of various high-voltage signal shapes and frequencies on the spinnability and productivity of polycaprolactone nano fibers*". Materials & Design, 213:110308, 2022.
   Impact Factor (2023): 7.6 (Q1). Citations: 62.

5. Sivan M, **Madheswaran D**, Asadian M, Cools P, Thukkaram M, Van Der Voort P, Morent R, De Geyter N and Lukas D "*Plasma treatment effects on bulk properties of polycaprolactone nanofibrous mats fabricated by uncommon AC electrospinning: A comparative study*". Surface & Coatings Technology,399:126203, 2020.
   Impact Factor (2023): 5.3 (Q1). Citations: 30.
   One of the images from this article has been featured in the cover page of the journal "Surface and Coatings Technology" 2020, 399.

5.1.1 The Web of Science or Scopus indexed Conference publications

1. **Madheswaran D**, Hauzerova S, Vatera J, Lisnenko M, Sivan M, Ondrej B, Jencova V, Lukas D, Frantisek J, Kostakova E.K *et al.* "*Braided threads with AC electrospun nanofibers for hygienic and medical applications*". Proceedings 13^{th} International Conference on Nanomaterials - Research & Application, 2022. Citations: 1.

2. Sivan M, **Madheswaran D**, Kalous T, Pokorny P, and Lukad D. "*Production of poly (ϵ-caprolactone) antimicrobial nanofibers by needleless alternating current electrospinning*". Materials Today: Proceedings, 17, 2019. Cite-score (2023): 4.9. Citations: 8.

5.1.2 Conferences

1. **Madheswaran D**, Sivan M, Valtera J, Lisnenko M, Caroline E, Lukas D, Kostakova E.K, "*Continuous fabrication of various braided composite nanofibrous surgical yarns using AC electrospinning and braiding technology*". 8^{th} International Conference on Electrospinning, 2024, Krakow, Poland.

2. **Madheswaran M**, Sivan M, Jencova V, Horakova J, Petr M, and Lukas D "*Analysis of HeLa Cell Migration using in vitro Scratch Assay by Image J*". 1^{st} Workshop on Mechanics of Nanomaterials, 2018, Czech Republic, ISBN: 978-80-7494-449-9.

3. Manikandan S, **Madheswaran D**, *et al.* "*Fabrication of poly(ϵ-caprolactone) Nanofibers using carboxylic acids by alternating current electrospinning*". 1^{st} Workshop on Mechanics of Nanomaterials, 2018, Czech Republic, ISBN: 978-80-7494-449-9.

4. Sivan M, **Madheswaran D**, Pokorny P, and Lukas D, "*Spinnability of poly (ϵ-caprolactone) using formic acid by needleless and collectorless alternating current electrospinning*". NANOCON, 2017, Czech Republic.

5. Kostakova E.K, Lukas D, Jencova V, Strnadova K, Sivan M, Jan V, **Madheswaran D**, Kristyna H, Sarka H, Lisnenko M, Vera H "*Characterisation of composite nanofibre yarns and their antimicrobial functionalization*". Biomaterials and their surfaces XVI, 2023, Czech Republic, ISBN: 978-80-01-07212-7.

6. Eva KK, David L, Jencova V, Strnadova K, Sivan M, Valtera J, **Madheswaran D**, Havlickova K, Hauzerova S, Lisnenko M, Vera H "*Study of degradation of composite yarns with nanofibre coating*". Biomaterials and their surfaces XVI, 2023, Czech Republic, ISBN: 978-80-01-07212-7.

Manuscripts under preparation

1. Madheswaran D, *et al.* "*The Continued Dominance of Sutures in Modern Surgery*" (Surgery, The editorial board has invited submissions for a commentary article).

2. M. Sivan, Madheswaran D, *et al.* "*Unlocking the potential of alternating current electrospinning in nanofiber production*"(Nanoscale, proposal was approved by the Editorial team for submitting review article).

3. Madheswaran D, *et al.* "*A review on advances in composite nanofibrous yarns: Fabrication techniques and emerging applications*".

4. Madheswaran D, *et al.* "*Fabrication of functional braided nanofiber-coated composite yarn for suture applications*".

6. Curriculum Vitae

Name	Divyabharathi Madheswaran
Address	341/103, Jestedska, Liberec 8
Date of birth	09/05/1991
Nationality	Indian
Email	divyabharathi.madheswaran@tul.cz

Education and Training

13/12/2016 – till now	Doctoral studies (Ph.D) Faculty of Textile Engineering Technical University of Liberec, Czech Republic
2012 – 2014	Post graduation (M.E Embedded systems) Faculty of Electrical Engineering Anna University,Chennai, India
2008 – 2012	Under graduation (B.E Electronics & Communication Engineering) Faculty of Information and Communication Engineering Anna University, Chennai, India
12/2018 – 3/2019	Internship Department of Applied Physics, Research Unit Plasma Technology Ghent University, Belgium
09/2019 – 12/2019	Internship Nanoprogress z.s Liberec, Czech Republic

7. Brief description of the current expertise, research and scientific activities

Doctoral Studies

Doctoral Studies	Textile Engineering Department of Nonwovens and Nanofibrous Materials
Specialization	Textile Technics and Materials Engineering - full time

List of Exam Passed

Nanofibres and Nanotechnologies
Macromolecular Chemistry
Tissue Engineering
Mathematical Statistics and Data Analysis
Experimental technique of the textile

State Doctoral Exam Completed on 21/06/2022 with the overall result passed

Teaching Activities

Winter/summer	Physical Principles of Nanofiber Fabrication
	Practical Course of Stereology

Projects

Research projects	Student Grant Scheme (SGS 21449) (Leader) Student Grant Scheme (SGS 21439, SGS 4481) (Member) PURE, TACR, GACR, AZV (Member) Technical University of Liberec, Czech Republic
	Cluster Nanoprogress z.s.

8. Recommendation of the supervisor

FAKULTA
PŘÍRODOVĚDNĚ-HUMANITNÍ
A PEDAGOGICKÁ TUL

Liberec, on 01/07/2024

Thesis: **FABRICATION AND CHARACTERIZATION OF SUTURES MADE FROM COMPOSITE NANOFIBROUS YARNS**

Author: Divyabharathi Madheswaran, M.Eng.

Supervisor's opinion

Divyabharathi Madheswaran's dissertation titled "Fabrication and characterization of sutures made from composite nanofibrous yarns" demonstrates the continuous fabrication of various antibacterial braided composite nanofibrous yarns and results of their subsequent analysis.

Divyabharathi's work is focused on several key experiments and methodologies: (i) She conducted experiments on pristine and Chlorhexidine (CHX)-loaded Polyamide6 (PA6) and Polyurethane (PU) electrospun fibers for the so-called sheath layer, with PA microyarns as the core. (ii) Next she investigated blends of Polycaprolactone and Polylactic acid (PCL-PLA), as well as PCL-PLA with CHX or Triclosan (TRC) for the sheath layer, using PLA micro-yarns as the core. (iii) Then she employed pristine PCL and PCL with CHX or TRC for the sheath layer and PLA micro-yarns for the core. (iv) Finally, she carried out morphological assessments that confirmed the successful fabrication of composite nanofibrous yarns and braided composite nanofibrous yarns. Using infrared spectroscopy, she verified the incorporation of antibacterial agents CHX) or TRC in the composite nanofibrous yarns. Divyabharathi demonstrated also a robust breaking force (29 N) and high thermal stability for braided CNYs. Additionally, she performed cytotoxicity and antibacterial tests, further underscoring the efficacy of the developed materials.

I can confirm that Divyabharathi has shown a deep interest in her chosen topic since the inception of her dissertation. The initial embarrassment with the ability of the doctoral student to work independently was soon dispelled and grew into an unusually high degree of self-invention, in-problem-finding, conducting experiments, critical evaluation, and subsequent successful publication of novel results.

The most significant outputs of her dissertation are: (i) The integration of AC electrospinning and braiding technologies, (ii) loading multiple functional components, such as antibacterial agents, into composite nanofibrous yarns, (iii) demonstration of efficiency and scalability for braided CNYs.

Divyabharathi has also identified recent limitations of composite nanofibrous yarns: (i) Weak adhesion between the electrospun fibrous sheath and the core yarn, which needs improvement to enhance the mechanical integrity of the sutures. (ii) Although the electrospinning process is efficient, the braiding process had a relatively low production rate of 0.25 m/min, which could limit large-scale manufacturing.

The findings from Divyabharathi's dissertation have been published in several high-impact, peer-reviewed international journals and proceedings (Web of Science and/or Scopus indexed):

- COMPOSITES COMMUNICATIONS (article, IF = 6.5, Q1)
- JOURNAL OF APPLIED POLYMER SCIENCE (article, IF = 2.7, Q2)
- MATERIALS TODAY CHEMISTRY (article, IF = 6.7, Q1)
- MATERIALS & DESIGN (article, IF = 7.6, Q1)
- SURFACE & COATINGS TECHNOLOGY (article, IF = 5.3, Q1)

David Lukáš | Head – Subdepartment Bioengineering | +420 485 353 146 | david.lukas@tul.cz
Technical University of Liberec | Faculty of science, humanities and education | Department of Chemistry
Studentská 1402/2, 461 17| web.fp.tul.cz

FAKULTA
PŘÍRODOVĚDNĚ-HUMANITNÍ
A PEDAGOGICKÁ TUL

- MATERIALS TODAY - PROCEEDINGS (SCOPUS INDEXED, Cite score = 4.9)
- NANOCON CONFRENCE PROCEEDINGS (SCOPUS INDEXED)

I rate the results of Divyabharathi Madheswaran thesis as excellent, which includes five international peer-reviewed articles with the Web of Science indexation. In addition, one more article is under the preparation. The value of her H-index is 5, with the sum of times cited 145.

Through her dissertation, Divyabharathi Madheswaran has provided a deeper understanding of nanofiber-based sutures, a critical biomaterial in healthcare. She attempts to show a way to groundbreaking advancements aimed at enhancing their multifunctionality or providing nanoscale fibrillar support for cellular activities. The development of these novel braided electrospun composite nanofibrous yarns offers potential improvements in the performance and therapeutic capabilities of sutures. Additionally, the use of AC electrospinning and braiding technology supports the industrial-scale production of these yarns, presenting a significant advantage.

I am convinced that Divyabharathi's research establishes a strong foundation for the development of next-generation surgical sutures and other biomedical materials, promising significant advancements in medical treatments and beyond.

Therefore, I propose that the work of Divyabharathi Madheswaran, M.Eng., be accepted for defense.

prof. RNDr. David Lukáš, CSc.

Appendix:

The analysis of plagiarism pointed out a 9% agreement with the thesis "Studies on the spinnability and surface modification of polycaprolactone nanofibers produced by AC electrospinning" (Author: Manikandan Sivan, PhD_Dissertation, Faculty of Textile Engineering - Technical University of Liberec).

A more detailed analysis of this match showed that 2223 words (out of a total of 4146 blue-marked matched words) belong to formal parts of the text, such as cover page, acknowledgements, list of abbreviations, materials and characterization, e.t.c., (Tab. 1).

Thus, the real value of the match is 9% x 0.46 = 4.1% of the total thesis words. Even this small amount can be excused by the multiple citations of M. Sivan's work in the text of the Divyabharathi Madheswaran's dissertation.

Despite of these findings, we have deeply discussed the ethical rules of scientific citations with Divyabharathi.

David Lukáš | Head – Subdepartment Bioengineering | +420 485 353 146 | david.lukas@tul.cz
Technical University of Liberec | Faculty of science, humanities and education | Department of Chemistry
Studentská 1402/2, 461 17| web.fp.tul.cz

FAKULTA
PŘÍRODOVĚDNĚ-HUMANITNÍ
A PEDAGOGICKÁ TUL

Tab. 1: 2223 words (out of a total of 4146 blue-marked matched words) belong to formal parts of the text, such as cover page, acknowledgements, list of abbreviations, materials and characterization, e.t.c.

Page. No	No. words (blue)	Excluding no. words	Remarks
2	73	73	Cover page
2	34	34	Cover page
4	69	69	Acknowledgements
8	30	30	List. Abbreviation
9	33	33	List. Abbreviation
10	97	0	Introduction
	78	0	
11	113	0	
22	160	0	
23	209	0	
23	90	0	
23	205	0	
24	79	0	
24	33	0	
24	27	0	
29	48	8	
31	67	9	
32	72	0	
32	74	0	
34	52	25	Materials
35	70	70	
35	58	5	
37	58	5	Characterization
38	195	0	
39	54	0	
40	68	0	
40	53	0	
40	106	0	
40	177	0	References
46	62	177	
50	75	62	
56	55	75	
58	342	55	
59	134	342	
60	115	134	
62	229	115	
63	60	229	
64	35	60	
66	578	35	
Total:	4167	578	
		2223	

David Lukáš | Head – Subdepartment Bioengineering | +420 485 353 146 | david.lukas@tul.cz
Technical University of Liberec | Faculty of science, humanities and education | Department of Chemistry
Studentská 1402/2, 461 17| web.fp.tul.cz

9. Opponents' reviews

Ph.D. Examiner's report on the Ph.D. thesis

FABRICATION AND CHARACTERIZATION OF SUTURES MADE FROM COMPOSITE NANOFIBROUS YARNS

Submitted by:

Divyabharathi Madheswaran, M.Eng.

to the Faculty of Textile Engineering of the Technical University of Liberec for the defence in partial fulfilment of the requirements for the Ph.D. graduation in Doctoral study program P3106 Textile Engineering, Doctoral study branch Textile Technics and Materials Engineering.

Ph.D. Thesis examiner **prof. Ing. et Ing. Ivo Kuřitka, Ph.D. et Ph.D.**

*****

The Thesis submitted by **Divyabharathi Madheswaran** consists of 120 pages of the main text and nineteen pages of obligatory formal parts, such as the table of contents, acknowledgements, abstract, lists of figures, tables etc.

The main text begins with an introductory chapter, which briefly defines the current state of the issue, highlights the importance of surgical site infections (SSI), and quickly focuses on the specific topic of sutures and their potential functionalization, which plays a role both in the problem and in its possible solution that should be found in the field of materials prepared by electrospinning. The dissertation builds on significant previous results, which it expands upon, and defines the research task to find a method for the fabrication of functional braided nanofibrous composite yarns. The approach is proposed for the first time in this PhD work. Hence a next generation of surgical sutures is ambitiously sought. It involves the initial creation of composite nanofibrous yarns using advanced AC electrospinning, followed by a second step utilizing braiding technology to enhance the overall mechanical properties and functionality of these yarns. The following subsection presents a logical breakdown of this goal into objectives, defining the activities and their purpose in solving the problem. Furthermore, the significance, structure, and research strategy of the dissertation are briefly introduced.

The second chapter provides the State of the Art in Literature in the field of surgical sutures. It is a very extensive general text, but at the same time rich in details and topical. This chapter is thoroughly prepared, combining information from both scientific publications and the commercial sector. The 40-page length is also substantial, and the chapter could easily serve as a chapter in a book. Will it also be published? I would only have one comment regarding the images taken from the literature, whether in addition to the citation, there should also be some indication about their licensing status.

Chapter 3, Materials and Methods, gives the reader a comprehensive overview of the materials and methods used to accomplish the goals of the dissertation. The materials are presented thoroughly; however, for the polymers, I would recommend including their dispersity ($Đ$) in addition to M_w. Surprisingly, chlorhexidine (CHX) is not mentioned in the second chapter, while triclosan (TRC) is, given that both antimicrobial agents are very common. I would have expected a mention of the choice of antimicrobial agents in the description of the third objective at the end of chapter 1.2. Of course, this does not diminish the significance of the work, which focuses on electrospinning technology as such. From this perspective, the choice of very common antibacterial agents is methodologically advantageous. I am curious whether the reference solutions were prepared under any special conditions, for example, filtered solvents or working in clean rooms, and if not, whether this caused any issues. The technology for the fabrication of composite nanofibrous yarns using AC electrospinning is described in the next part of the text, followed by the description of the fabrication of braided composite nanofibrous yarns. I wonder what is meant by the word "composite" in the term "composite nanofibrous yarn." The descriptions of the characterization methods are appropriately brief, but the description of the abrasion test is detailed, which is great since it is not a commonly known method. The part of the test involving testing the nanofibrous envelope during sewing, which the author developed independently, could be expanded to include a description of how the results are evaluated, and not just the procedure. The inhibition zone tests for antibacterial activity have somewhat limited value in relation to polymeric materials, where one would expect surface antimicrobial activity, as it raises the question of what exactly is being tested and what does this test indicate? However, in the initial assumption that the material should release an antimicrobial agent, and the larger the zone, the better, these tests have sufficiently indicative value. Cytotoxicity was tested in the standard way using an extract from the material in the culture medium. Prior to that, the samples were sterilized with ethylene oxide. Are other sterilization methods also considerable?

Chapter 4 presents the results of the work. Appropriately, it is stated at the beginning that these results have already been published in two articles in peer-reviewed journals. In both cases, the dissertation author is the first author. However, it would be helpful to specify the author's level of contribution to these publications. Since the results have already gone through the peer review process, it is not necessary to analyze them in detail.

In the first subchapter, the study focuses on the fabrication of chlorhexidine-loaded PU and PA6 composite nanofibrous yarns.

Some notices: The graphs in Figure 4.2 would be more readable with larger fonts; values such as 22.0 ± 1.1 mg/L should preferably be written in parentheses (22.0 ± 1.1) mg/L; in the sentence "The first three atoms can be expected based on the chemical structure of the polymer, ..." it would be more appropriate to use "elements" instead of "atoms."

The comparison between XPS and HPLC results is interesting. I would ask the author to consider whether the difference could be due to the varying concentration of CHX on the

surface versus in the bulk of the fiber. Additionally, would the HPLC analysis yield the same result if the sample underwent the same vacuum history as the sample in the XPS analysis? I appreciate the subsections on mechanical and thermal properties. In the subsections on biological properties, the differences between the prepared materials as well as the properties of individual testing methods are properly reflected.

The second part is about the continuous fabrication of functional braided PLA core PCL-PLA sheath composite nanofibrous yarns, which is a well-elaborated study. Some observations: Here, Figure 4.9 is clearly readable; the incorporation of CHX or TRC in the resultant braided yarn seems to be clearly indicated by the results, without the need for complex explanations. Regarding biological properties, we again see that a material excelling in the diffusion zone test will also fail in cytocompatibility if non-specific antibacterial agents are used. From the perspective of antimicrobial properties, the ideal polymeric material would be one from which nothing is released into the surroundings, yet no microorganism survives or adheres to its surface.

The third subsection, continuous fabrication of functional braided PLA core PCL sheath composite nanofibrous yarns, represents another stage in the development of surgical sutures. The work approaches application, and here we finally see the results of the abrasion test. In the biological tests, the best result was achieved by the sample TRC-loaded braided PLA/PCL CNY, which demonstrated superior antibacterial activity and better cytocompatibility. The text suggests that this indicates promise for infection control, and this marks the culmination of the work. For further research, it could be recommended to consider anchoring of the antimicrobial additive within or on the surface of the polymer.

Chapter 5 summarizes the results and conclusions of the work in points and highlights the strengths and weaknesses of the achieved results. The future work outlook is set out in a manner consistent with what has been achieved. Appendices and a bibliography follow, with appropriate quantity and relevance of used resources.

*****

Further, in addition to the review above, a summary and additional comments on specific points are provided.

a) Assessment of the significance of the dissertation for the field of study

The dissertation represents progress in the field of study of, bringing new insights, new ideas, and their implementation. New insights were gained in the research and development of materials for AC electrospinning and braiding technology, as well as in the effect of the processing method on the properties of the final product. The research and development of sutures composed of an electrospun sheath layer with incorporated antimicrobial or other functional additives, and a core yarn providing the necessary mechanical properties, may enable future innovation in the use of studied technologies. The problem of SSIs is serious, and any contribution to its solution is valuable. This work has

demonstrated a result that, although not yet directly applicable in medicine, represents a step toward such application and serves as a good starting point for the development of a new type of surgical sutures.

b) Evaluation of the approach to problem-solving, methods used, and achievement of the goal of the dissertation

The goal of the dissertation has been achieved. The problems were reasonably defined, and it was clearly outlined what had been accomplished before and what the work builds upon. The work breakdown structure was then translated into objectives with verifiable outputs. The experimental methods were appropriately chosen and are adequate for solving the defined problems. In addition to standard methods, the author also designed original test for the nanofibrous envelope during sewing. Some might consider it naive and overly simple, but I appreciate it as a test clearly aimed at assessing real-world conditions, or at least approaching it, and providing some insight into the application potential of the prepared surgical suture.

c) Opinion on the results of the dissertation and the significance of the author's original and specific contribution

Chapters 3, 4, and 5, which describe the materials, methods, present and discuss the results, and summarize the conclusions, form the core of the dissertation, spanning 50 pages, which is sufficient. The results are original, and they contributed to the field. The results contained within the dissertation have been published in peer-reviewed journals (Q1 and Q2) and have already begun to receive citations. The author's contribution and its importance are further highlighted by the first position of the doctoral student among co-authors of both publications.

d) Any further comments, especially regarding the systematic approach, clarity, formal arrangement, and language quality of the dissertation

The literature survey and state of the art description is conducted thoroughly and will be useful to readers, even if they only read this part.

e) Evaluation of the doctoral student's publications

In addition to the two publications in Q1 and Q2 journals that form the core of the dissertation, for which the doctoral student is the first author, the student has also published three additional works as a second co-author and has more than sufficient experience in presenting at conferences. The author also mentions three manuscripts in preparation, all of them in the topic of the dissertation, which suggests a broader involvement in the work of the home research institution. The quality of the author's publications, and certainly that of the entire team, is best evidenced by the fact that, with five publications, the author's h-index is 5.

f) Clear statement from the reviewer on whether they recommend or do not recommend the dissertation for defence

I recommend the dissertation for defence.

*****

Verdict of the examiner:

In my opinion, the submitted Thesis fulfils all requirements imposed on a PhD thesis. Therefore, I recommend the Thesis for defence, and upon successful defence Divyabharathi Madheswaran, M.Eng., to be awarded a doctoral degree, i.e. the title "Doctor of Philosophy Ph.D.".

In Zlín, 29th September 2024

Ivo Kuřitka

prof. Ing. et Ing. Ivo Kuřitka, Ph.D. et Ph.D.
Centre of Polymer Systems
University Institute
Tomas Bata University in Zlín
tř. Tomáše Bati 5678
Zlín 760 01
Czech Republic

Dissertation Review

Title of dissertation: **Fabrication and Characterization of Sutures Made from Composite Nanofibrous Yarns**
Dissertation Author: **Divyabharathi Madheswaran, M.Eng.**
Field of study: Textile Engineering

The significance of the dissertation for the field
This dissertation deals with solving research gaps and designing innovative solutions for the development of a functional braided composite nanofibrous yarns (CNY) that will be used to make surgical sutures to close the wound while also carrying the necessary therapeutic agent for healing. The microscale CNYs were fabricated using alternating current (AC) at a speed of 30m / min. This technique was developed by the team of Prof. David Lukáš, a supervisor of this thesis. The fabricated CNYs were braided to enhance their mechanical properties, where the microfiber core provided mechanical support for wound closure, while the fibrous sheath mimicked the ECM and facilitated the cell activities and allowed the incorporation of antibacterial agents - chlorhexidine (CHX) or triclosan (TRC) to accelerate healing. Several polymers PU and PA6 with PA6 as core and PCL-PLA blends with PLA as core and PCL with PLA as core were used. The polymers were either neat or impregnated with CHX or TRC. The prepared products were characterized using morphological assessments, FTIR, mechanical tests, thermal analysis and antimicrobial and cytotoxicity tests.
As a primary objective, a new approach to fabricate functional braided CNYs by AC electrospinning and braiding technology was developed, leading to a coating of microyarns with nanofibers by AC electrospinning and subsequent braiding of CNYs to create braided CNY structures applicable for surgical structures. Another goal was a complete evaluation of as-fabricated yarns using various physicochemical, morphological, thermal and mechanical test methods as well as antimicrobial activities and biocompatibility which support cellular activities critical for wound healing.
The significance of the dissertation lies in two important directions. 1) the use and verification of a new method based on AC electrospinning in order to produce functional surgical threads and 2) the preparation of a new type of surgical thread, with better functional properties allowing to reduce the risk of infection, improve cellular interactions, improve mechanical properties and so on. In times of antimicrobial resistance and the threat of increased infections, the chosen topic is very current and necessary. Research in this area is very widespread and the contribution of the TUL team is very significant in this area.

The procedure for solving the problem, the methods used, the fulfillment of the set goal
As already mentioned, the AC electrospinning method was used for the production of the proposed CNYs, followed by braiding of CNYs to braided CNY structures. The list of various characterization techniques is sufficient (SEM, FT–IR, XPS, linear density measurement, mechanical property testing, TGA analysis, abrasion testing, cytotoxicity testing, HPLC analysis and antibacterial testing) and enables determining the required properties of the prepared materials. The set goals were met in full.

Opinion on the systematicity, clarity, formal arrangement and language level of the dissertation

The dissertation is written in a very comprehensible, readable manner, includes all the necessary parts, starting with lists of figures, tables, abbreviations and symbols and continuing with an overview of the current state of knowledge, which is focused on commercial surgical suture technologies and fabrication methods with an explanation of the principles, advantages and disadvantages and differences of DC and AC electrospinning processes. This is followed by a chapter on the materials used and a description of the methods used for experimental preparation and characterization. Then the chapter Obtained results and Conclusion is inserted and completed with references (there is a small deviation here, the chapter in the content is called References, in the text Bibliography). The number of citations reaches 150, sometimes there is a small error (e.g. fonts in the citation [29]), many of them are from the last 5-6 years or even older.

Chapter 2 is focused in detail on focused on surgical sutures and electrospinning-based yarn sutures fabrication, including a description of the device developed at TUL in the team of prof. David Lukáš, and a description of the braiding process. The text is supplemented with numerous figures and schemes that adequately describe the mentioned processes, **but some of them should have been larger for better readability.** The thesis has a logical structure, clear presentation and discussion of the results.

Publications

The results of this dissertation were published in two articles (the author is the first author), however, the author further also listed other publications reaching the total of 5 publications, as well as 8 conference contributions and 3 other upcoming publications. Thus, the author is therefore very active and has the perspective of a successful research career.

Comments and questions

1. As previously stated, the figures and diagrams in Chapter 2 are difficult to read due to the font size.
2. Chapter 3 describes the preparation of polymer solutions in a certain % content, on the basis of which were these quantities or ratios selected?
3. On the basis of which parameters were chosen for AC electrospinning, which are listed in table 3.2?
4. Why were the methods used: 1) sewing yarns to a silicone mold and 2) sewing yarns to a silicone mold with a drop of PBS? Chicken leg is understandable.
5. Figure 4.1 g,h – Could you explain the molecular interactions of CHX with the PU and PA6 chains?
6. On the same page, there is an incorrect reference to Figure 4.13c and g.
7. What was the source of the Ca contamination visible in Figure 4.2?
8. Was CHX homogeneously distributed in PU or PA6?
9. The names of bacterial strains appear several times in the text, they are not written, as is usual, in italics, e.g. p. 73, 82.
10. How do you explain that PA6-CHX CNYs and PLA/PCL-PLA-CHX were biocompatible and PLA/PCL-CHX did not perform well, on the contrary PLA/PCL-TRC was much better?

Opinion on the results of the dissertation and the importance of the original contribution of the author of the thesis

The addressed topic corresponds to current research trends in the area of smart surgical materials. It brings new technology for the production of surgical sutures with improved functional properties leading to more effective wound treatment. The application of AC electrospinning is interesting, but it is not clear from the work whether the author used this method already developed as a tool for her research, or whether she participated in the development of this technology herself.
The submitted dissertation fulfilled the defined goals. The author has demonstrated the ability to work independently. The results of this work have been published and are a significant contribution to the development of new materials for surgical sutures. At the same time, it pointed out the limitations of the methods of AC electrospinning and braiding process used for the production of braided CNYs. Considering the above, I consider the work to be very well done and

I recommend the dissertation for defense and in the case of a successful defense award the PhD degree.

Ostrava, 29 August 2024

Prof. Ing. Daniela Plachá, Ph.D.